श्री चित्रा तिरुनाल आयुर्विज्ञान और प्रौद्योगिकी संस्थान, त्रिवेंद्रम, तिरुवनन्तपुरम - 695 011, केरल, भारत
SREE CHITRA TIRUNAL INSTITUTE FOR MEDICAL SCIENCES AND TECHNOLOGY, TRIVANDRUM
THIRUVANANTHAPURAM - 695 011, KERALA, INDIA
(एक राष्ट्रीय महत्व का संस्थान, विज्ञान और प्रौद्योगिकी विभाग, भारत सरकार)
(An Institution of National Importance, Department of Science and Technology, Government of India)
टेलीफोन नं./Telephone No.: 0471-2443152 फैक्स/Fax: 0471-2446433, 2550728
ई-मेल/E-mail: sct@sctimst.ac.in वेबसाइट/Website: www.sctimst.ac.in

PROJECT COMPLETION REPORT

1. **Project number:** 5137
2. **Title of the project:** Mechanisms of anticancer activity of emodin/aloe emodin: effects on cell growth, angiogenesis and metastasis in human colon cancer cells
3. **Funding Agency Name:** Department of Atomic Energy, BNRS
4. **Project Reference Number provided by the Funding Agency:** 2003/37/32/BRNS/1989
5. **Principal Investigator (Name & Address):**

Dr. Srinivas G
Scientist D
Department of Biochemistry
Sree Chitra Tirunal institute for Medical Science and Technology
Thiruvananthapuram 695 011
Kerala

6. **Co-Investigators (Name & Address): Dr. Priya Srinivas, Scientist B, Cancer Biology, RGCB, Trivandrum 695014**
7. **Implementing Institution:** SCTIMST
8. **Collaborating Institutions:** Nil
9. **Date of Commencement**: 31/10/2004
10. **Duration**: 2 Years
11. **Date of completion**: 10/12/2006
12. **Objectives as approved**:

1) To study the in vitro antiproliferative effects of emodin/aloe emodin in human colon cancer cell lines by MTT assay and Thymidine incorporation.
2) To elucidate the mechanism of action of cell death of emodin/aloe emodin in human colon cancer cells by annexin-FITC staining, TUNEL assay, Comet assay, spectrofluorimetric assay for caspase activation and western blotting.
3) To evaluate the inhibition of angiogenesis by emodin in an *in vitro* angiogenesis assay.
4) To assess the metastasis inhibitory activity of the drug with respect to cell migration (by cell invasion assay), MMP inhibition (ELISA) and associated gene expression.

5) To assess the role emodin in regulating iNOS, MMPs and TIMPs by Western Blotiing/ RT-PCR.

13. **Deviation made from original objectives if any, while implementing the project and reasons thereof:** NA

14. **Field/Experimental work giving full details of summary of methods adopted, data collected supported by necessary tables, charts, diagrams and photographs**:

Methodology

MTT–cell proliferation assay

This assay was done for emodin/aloe emodin as per standard protocol. Human colon cancer cells (SW 480, SW620 and HCT 116) were used for the study.

Apoptosis assays

a) Annexin-PI staining

As apoptosis causes changes in membrane permeability, there is a flip-flop of phosphatidylserine to the outer membrane, which is considered to be one of the early markers of apoptosis.

b) TUNEL assay

Briefly, the cells were grown in cover slips and treated with the appropriate concentrations of the compounds with and without the drugs. After washing with PBS, 100 ul of TdT reaction were added to the sections on the slide and then incubated at 370C for 60 min inside a humidified chamber for the end labelling reaction to occur.

c) Comet assay

For this, the cells after treatment were pelletted and resuspended in 0.5 % low melting point agarose at 370C and layered on a frosted microscope slide previously coated with a thin layer of 0.5 % normal melting agarose and was kept for 5min at 40C. After that the slides were electrophoresed for 20 to 60 min at 25 V. The slides after electrophoresis were washed with 0.4 M Tris (pH 7.5) and stained with ethidium bromide and observed under a fluorescent microscope.

Mitochondrial Membrane Potential (MMP) assay

Mitochondrial membrane potential was measured by using ApoAlert Mitochondrial Membrane Sensor Kit as described by the manufacturer (Clontech Laboratories Inc.,

Mountain View, CA, USA). Briefly, after 12 h treatment with 12.5 µM of aloe emodin, the cells were treated with mitosensor reagent and incubated for 20 min.

Flow cytometric analysis

For flow cytometric analysis of cell cycle, cells were treated with 30 µM of aloe emodin for 48 h and harvested in 70% ice cold ethanol. Cells were then resuspended in 0.5 mg/ml RNase A for 1 h at 37°C. DNA was stained using 10 µg/ml propidium iodide and analyzed using FACSAria Flow Cytometer (BD Biosciences, San Jose, CA, USA). The percentage of cells in different cell cycle phases (G0, G1, S or G2/M) were calculated using FACS Diva DNA Analysis Software.

Caspase -3/7 and Caspase -9 assay

Activation of caspases 3/7 and caspase -9 was determined using Caspase-Glo 3/7 Assay and Caspase-Glo 9 Assay Kit (Promega Corporation, Madison, WI, USA). The cells were treated with varying concentrations of aloe emodin and after treatment, 100 µl of Caspase-Glo 3/7 reagent was added and incubated for 2 h at room temperature. Luminescence was measured with Sirius Single Tube Luminometer (Berthold Technologies GmbH & Co. KG, Bad Wildbad, Germany). Relative Luminescence Units (RLUs) were calculated after normalizing with the protein content.

Caspase -6 assay

Activation of caspase -6 was determined using Caspase -6 Fluorometric Assy Kit (Abcam, Cambridge, UK). Cells were treated with different concentrations of aloe emodin for 24/48 h and after treatment, resuspended in 50 µl of chilled cell lysis buffer. Then 50 µl of 2X reaction buffer containing 10 mM Dithiothreitol (DTT) and 50 µM VEID-AFC substrate were added. After 2 h incubation fluorescence was measured (400 nm excitation wave length and 505 nm emission wave length) with FLx800 Fluorescence Microplate Reader (BioTek instruments, Winooski, VT, USA).

Western blot analysis

After treatment the cells were lysed in ice-cold Radio Immuno Precipitation Assay (Rai et al.) buffer and proteins were resolved on Sodium Dodecyl Sulphate- Poly Acrylamide Gel Electrophoresis (SDS-PAGE), transferred to nitrocellulose membrane and probed with antibodies to PARP, procaspase -3, procaspase -7, procaspase -9, cleaved caspase -3, cleaved

caspase -7, cleaved caspase -9, caspase -6, cyclin B1, phosphoERK1/2, phosphoJNK1/2, phosphop38, RhoB, NF-κB, IκB, histone and β- actin. Horseradish Peroxidase (HRP) conjugated secondary antibodies (anti rabbit IgG, anti mouse IgG and anti goat IgG) were used and the bands were visualized as per the protocols given in the West Pico Chemiluminescence Detection Kit (Pierce Biotechnology Inc., Rockford, IL, USA). Bands were documented in Gel Doc™ XR Imaging System (Bio-Rad Laboratories, Hercules, CA, USA) and quantified using Quantity One 1 D Analysis Software.

Semi Quantitative RT-PCR and real time RT-PCR analysis of MMP-2, MMP-9 RhoB and VEGF- A

After treatment with aloe emodin, total RNA was isolated using Pure Link RNA Mini Kit (Invitrogen Corporation, Carlsbad, CA, USA) following manufacture's protocol. The cDNA was synthesized with 4 µg of total RNA using Moloney Murine Leukemia Virus Reverse Transcriptase (MMLV-RT) and random primers (Promega Corporation, Madison, WI, USA). PCR was done with specific primers using iCycler Thermal Cycler (Bio-Rad Laboratories, Hercules, USA). β- actin, a non-regulated housekeeping gene was used as an internal control to normalize input cDNA. The real time PCR was performed by 1 µg of cDNA and 2 pM primers per reaction in 7900 HT Fast Real-Time PCR system (Applied Biosystems, Carlsbad, CA, USA) using MESA green qPCR Mastermix for SYBR Assay (Eurogentec, Seraing, Belgium).

Table 1. Sequence of forward and reverse primers used for PCR amplification

Gene	Primer sequence	Product size
MMP1	5'-GAGCAGATGTGGACCAT-3' 5'-ACCGGACTTCATCTCTGTCG-3'	645bp
MMP-2	5'-CAGGCTCTTCTCCTTTCACAAC-3' 5'-AAGCCACGGCTTGGTTTTCCTC-3	400bp
MMP-9	5'-TGGGCTACGTGACCTATGACAT -3 5'-GCCCAGCCCACCTCCACTCCTC -3'	173bp
MMP 3	5'-CTCACAGACCTGACTCGGTT-3' 5'-CACGCCTGAAGGAAGAGATG-3'	294bp
MMP 7	5'-TACAGTGGGAACAGGCTCAGG-3' 5'-GGCACTCCACATCTGGGCT-3'	181bp
MMP8	5'-TGGACCCAATGGAATCCTTGC-3' 5-'ATAGCCACTCAGAGCCCAGTA-3'	544bp
MMP10	5'-CGACAGAAGAGGTTCGTGCT-3'	209bp

	5’-CTTGGATAACCTGCTTGTACCTCAT-3’	
MMP11	5’-CGACAGAAGAGGTTCGTGCT-3’ 5’-CTTGGCTGCTGTTGTGTGTGCT3’	710bp
MMP 13	5’-AAGATGCATCCAGGGGTCCT-3’ 5’-GTCCAGGTTTCATCATCATCA-3’	626bp
MMP 15	5’-CCATATGTCCACCATGCGTT-3’ 5’-ATGATGGCATTGGGGTTGCT-3’	627bp
TIMP1	5’-GGGGACACCAGAAGTCAACCAGA-3’ 5’-CTTTTCAGAGCCTTGGAGGAGCT-3’	400bp
TIMP2	5’- GTTTTGCAATGCAGATGTAG-3’ 5’-ATGTGGAGAAACTCCTGCTT-3’	540bp
Rho A	5’-ATGGCTGCCATCCGGAAGAAA-3’ 5’-TCACAAGACAAGGCAACCAGA-3’	582bp
RhoB	5’-GCGTGCGGCAAGACGTCTG-3’ 5’-TCATAGCACCTTGCAGCAGTT-3’	548bp
Rho C	5’-ATGGCTGCAATCCGAAAGAAG-3’ 5’-TCAGAGAATGGGACAGCCCCT-3’	582bp
Rac 1	5’-CATCAAGTGTGTGGTGGTGGG-3’ 5’-TTACAGCACCAATCTCCTTAG-3’	448bp
Ki Ras	5’-AGCCTGTTTTGTGTCTACTGTT-3’ 5’-GAGAGGCCTGCTGAAAATG-3’	405bp
VEGF-A	5’-ATCTGCATGGTGATGTTGGA-3’ 5’-GGGCAGAATCATCACGAAGT-3’	218bp
β- actin	5’-TGGCACCACACCTTCTACAA-3’ 5’-GCACAGCTTCTCCTTAATGT-3’	396bp

Cyclin B1, MMP-2/9, RhoB and VEGF promoter activity assay

The cyclin B1-promoter firefly luciferase reporter construct was obtained as kind gift from Dr. Kurt Engeland (University of Leipzig, Leipzig, Germany) (Wasner et al., 2003). MMP-2 and MMP-9 luciferase reporter plasmids were obtained from Dr. C. D. Kim (Pusan National University, Busan, Korea), and Dr. Douglas D. Boyd (MD Anderson Cancer Center, Houston, USA), respectively (Lee et al., 2008; Liang et al., 2009; Sato et al., 1993). RhoB reporter plasmid was gifted by Dr. Misun Won, Medical Genome Research Center, Kribb, Daejeon, Korea (Kim et al., 2010). VEGF luciferase promoter was given by Dr. G. Pages (Institute of Developmental Biology and Cancer, Nice, France) (Maussang et al., 2006). The cells were grown to 70% confluency and

transfected with pRL-Null (Promega Corporation, Madison, WI, USA), cyclin B1/MMP-2/9/RhoB/VEGF luciferase reporter plasmids using Metafectene (Biontex Laboratories GmbH, Planegg, Germany). After transfection, the cells were treated with and without 20 μM aloe emodin/ PMA (100 ng/ml) and luciferase reporter assays were performed by Dual Luciferase Reporter Assay System (Promega Corporation, Madison, WI, USA) following the manufacturer's protocol and luciferase activity was measured by Sirius Single Tube Luminometer. Fire-fly luciferase activity was normalized for transfection efficiency using Renilla Luciferase activity (pRL-null) and protein content.

MMP-2/9 activity assay

Gelatinolytic activity was analyzed by using Innozyme Gelatinase MMP-2/9 Activity Assay Kit (Merck KGaA, Darmstadt, Germany). Culture supernatant, collected after 24 h aloe emodin treatment (10- 40 μM) with and without PMA, after concentration, was incubated with activation buffer and substrate working solution for 6 h at 37oC. MMP-2/9 is exclusively released in their inactive proforms and, therefore, detection of MMP-2/9 activity required preincubation with the synthetic MMP-2/9 activator p-AminoPhenyl-Mercuric Acetate (APMA). Fluorescence was measured at excitation wavelength of 320 nm and emission wavelength of 405 nm in Microplate Reader (Tecan, Mannedorf, Switzerland) and analyzed using MagellanTM Software.

Gelatin zymography

Cells were seeded into the 60 mm plate and treated with 100 ng/ml PMA and different concentrations of aloe emodin (10- 40 μM) for 24 h. Subsequently, the conditioned medium was collected, concentrated and gelatin zymography were performed with slight modifications to examine the activities of MMP-2 and MMP-9 (Kim et al., 2008). Briefly, samples were mixed with loading buffer and electrophoresed on 8 % SDS-polyacrylamide gel containing 0.1% gelatin. After incubating at 370 C for 24 h in zymography reaction buffer the gel was stained with Coomassie blue R-250 for 1 h and destained. Non-staining bands represents the levels of the active form of MMP-2 and MMP-9. Clear bands were documented in Gel Doc™ XR Imaging System and the inverted images were quantified by densitometric measurement using Quantity One 1 D Analysis Software.

Electrophoretic Mobility Shift Assay (EMSA)

The DNA binding activities of NF-κB in nuclear extracts were assessed by Electrophoretic Mobility Shift Assay (EMSA) (Chen et al., 2008) with slight

modifications using the LightShift Chemiluminescence EMSA kit from Pierce Biotechnology Inc. (Rockford, IL, USA). Nuclear proteins were extracted from cells using NE-PER nuclear and cytoplasmic extraction reagents (Pierce Biotechnology Inc., Rockford, IL, USA). Complementary oligonucleotide probes containing the NF-κB and AP1 binding motifs (NF-κB -5' probe, 5'-TTGTTACAAGGGACTTTCCGCTGGGGACTTTCCAGGGAGGCGTGG-3', NF-κB- 3' probe, 5'-CCACGCCTCCCTGGAAAGTCCCCAGCGGAAAGTCCCTTGTAACA- 3', AP1 5' probe, 5'- CGCTTGATGACTCAGCCGGAA- 3', AP1 3' probe, 5'-GCGAACTACTGAGTCGGCCTT- 3') were end labelled with biotin using Biotin 3' End Labelling Kit (Pierce Biotechnology Inc., Rockford, IL, USA) according to the manufacturer's protocol. Nuclear protein extracted after treatment with aloe emodin/PMA was incubated with 20 fmol of biotin-labelled oligonucleotide for 20 min at room temperature in 1X binding buffer. Products of binding reactions were resolved by electrophoresis on a 6% polyacrylamide gel using 0.5X Tris-Borate EDTA (TBE) buffer. Protein-oligonucleotide complex was electroblotted and UV crosslinked to a Biodyne B Pre-Cut Modified Nylon Membrane (Pierce Biotechnology Inc., Rockford, IL, USA). After blocking, the membrane was incubated with streptavidin-HRP conjugate. Detection of protein-oligonucleotide complex was performed according to the manufacturer's protocol. DNA probe bound with protein migrate slowly in gel compared to the free probe (FP) which migrate faster and appear at the lower side of the gel. Band intensity of protein-oligonucleotide complex was documented in Gel Doc™ XR Imaging System.

Scratch wound healing assay

Cells were pre-incubated for 24 h in serum-free DMEM before creating a wound across the cell monolayer with a plastic tip. After creating a wound, cells were treated with aloe emodin/PMA. Cell migration into the wound surface was then measured after 24 h using ProgRes CapturePro V2.8.0 Software and reported as the width of the remaining wounded area relative to the initial wound area (in micrometers). A known migration inducing agent, PMA was used to induce migration.

Cell migration/invasion assay

Migration of WiDr cells were determined by modified Boyden's chamber method using culture inserts of 8 μm pore size. Cells were seeded into the upper well of each chamber with and without aloe emodin and 500 μl of DMEM with 10% FBS was added to the

lower chamber. Migration was induced by 100 ng/ml of PMA. Cell migration was assayed by counting the number of cells that had migrated from the upper side to the lower side of the membrane after 24 h of incubation. Migrated cells were fixed with cold methanol and stained with 0.5% Crystal Violet solution. We used BioCoat Matrigel Invasion Chambers for assessing cell invasion instead of empty cell culture inserts (BD Biosciences, Bedford, MA, USA).

In vitro tube formation assay

Human Umbilical Vein Endothelial Cells (HUVECs) when plated on Matrigel, align themselves to form tubes like structures. For this assay 500 µg of Matrigel (BD Biosciences, Bedford, MA, USA) was coated on the wells of 96 well plate and incubated for 30 min at 37oC to solidify the gel. 1.5X103 HUVECs were then plated on the Matrigel and cultured in DMEM containing 25 µM of aloe emodin for 24 h. The enclosed network of complete tubes were observed and photographed.

Statistical analysis

All statistical calculations were carried out with the GraphPad Prism Software (version 5 for Windows). Values are expressed as the mean ± Standard Deviation (SD). The differences among the mean values from at least three independent experiments were analyzed with one-way ANOVA followed by Tukey's post hoc t-test analysis. The significance of the difference from the respective control for each experimental test conditions was assayed by Student's t-test for each paired experiment. Differences between means were considered statistically significant at $P < 0.05$.

15. Detailed analysis of Results

Growth inhibitory activity of aloe emodin

In this section we explain the growth inhibitory activity of aloe emodin and the possible mechanism for its antiproliferative effect. Our results show that aloe emodin repressed the proliferation of cancer cells in a concentration dependent manner. It is also shown that the growth inhibitory effect was brought about by a cell cycle arrest by modulating various molecules associated with cell cycle regulatory machinery.

Aloe emodin inhibits proliferation of colon cancer cells

Preliminary information about the cytotoxicity of aloe emodin and emodin was determined by measuring the activity of enzyme that reduces MTT to formazan after the addition of control medium or various concentrations of aloe emodin/emodin. This assay is based on measuring total cell kill of both proliferating and non-proliferating cells and in fact, measures the end effect of drug action. Both compounds inhibited the proliferation of all the colon cancer cell lines studied, WiDr, SW 480, SW 620 and RKO, in a concentration dependent manner (Figure 1, 2).

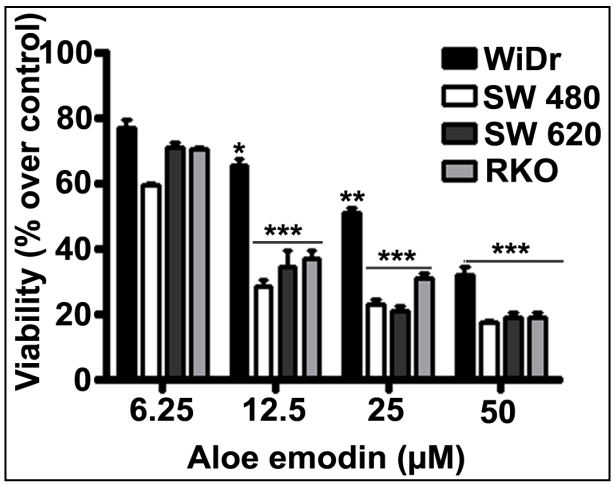

Figure 1. Analysis of cell viability in aloe emodin treated cells

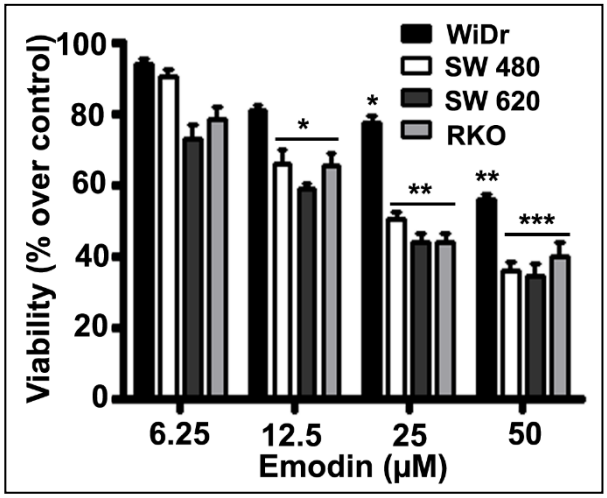

Figure 2. Analysis of cell viability in emodin treated cells

Role of ROS in aloe emodin induced antiproliferative activity

There are several reports showing both aloe emodin and emodin inducing reactive oxygen species dependent cell death mechanisms in variety of cells. Therefore, we analyzed whether the inhibition of proliferation in WiDr colon cancer cells was mediated through the activation of reactive oxygen species by using known free radical scavengers, Pyrrolidine Dithiocarbamate (PDTC) and N-Acetyl-L-Cysteine (NAC). These two compounds are powerful antioxidants and are known to inhibit the formation of reactive oxygen species by more than one mechanism. Both antioxidants were unable to provide a protective effect for the antiproliferative activity of aloe emodin/emodin (Figure 3, 4).

Figure 3. Effect of NAC and PDTC in aloe emodin induced cell death

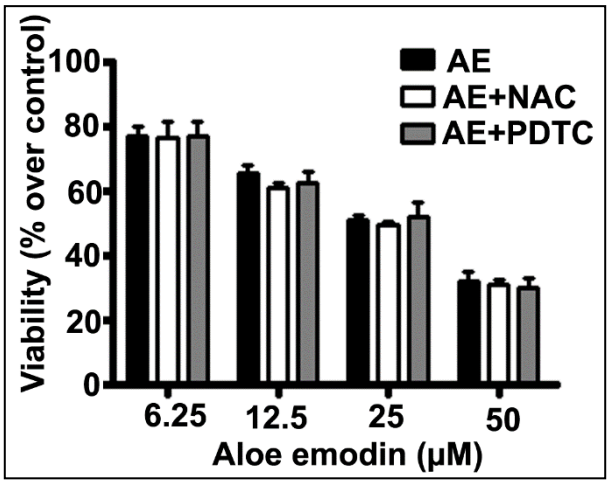

Figure 4. Effect of NAC and PDTC in emodin induced cell death

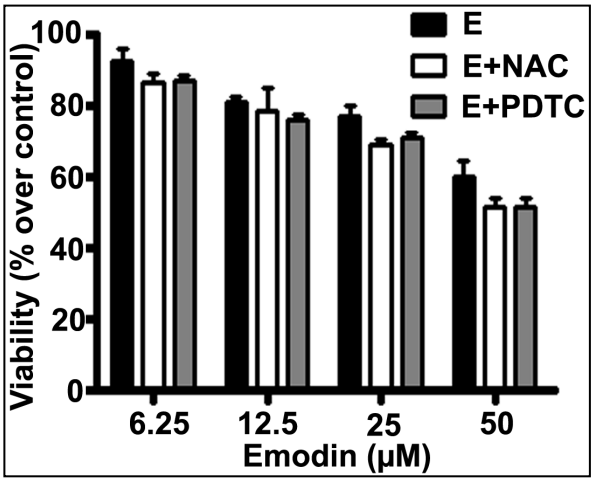

This suggests that aloe emodin/emodin exerts their antiproliferative effect without eliciting oxidative stress in WiDr cells. Toxicity of a compound is represented as LD_{50} values (Lethal

Dose, 50%; or Median Lethal Dose), a measure of the concentration needed to kill 50% of the cells. LD_{50} values derived from MTT assay for aloe emodin/emodin for the cell lines studied is shown in Table 2.

Table 2. LD_{50} values of aloe emodin/emodin

	LD_{50} (µM)			
	WiDr	SW 480	SW 620	RKO
Aloe emodin	28.9	11	9	27.9
Emodin	46	38.5	24	36

When compared the effect of emodin and aloe emodin on viability of colon cancer cells, aloe emodin was found to be more cytotoxic and effective among the panel of cell lines, hence we selected aloe emodin for further validating its antiproliferative effect in WiDr colon cancer cells.

Aloe emodin induces cell cycle arrest at G2/M phase and modulates cell cycle regulatory proteins

Induction of cell cycle arrest at G2/M

We checked whether aloe emodin induced cell growth inhibition was due to perturbation of cell cycle. Cell cycle analysis was done in a BD Biosciences FACSAria Flow Cytometer and representative histograms obtained are depicted in Figure 5.

Figure 5. Histograms of flow cytometric analysis of cell cycle

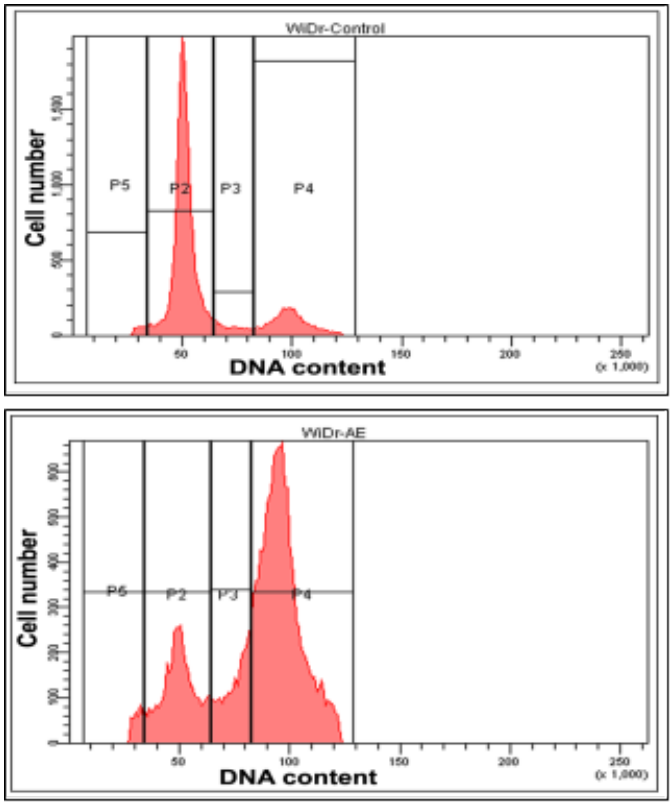

Distribution of cells in untreated cells were G0 (1.6%), G1 (76.4%), S (5.0%), G2/M (16.7%). In cells treated with 30 µM aloe emodin for 48 h, cell cycle distribution was G0 (2%), G1 (20.3%), S (12%), G2/M (64.2%). Cell phase distribution analysis showed a 3.8 fold increase in number of cells at G2/M phase upon treatment with aloe emodin with a corresponding decrease in number of cells distributed at G1 phase (Figure 6).

Figure 6. Analysis of cell cycle after treatment with aloe emodin

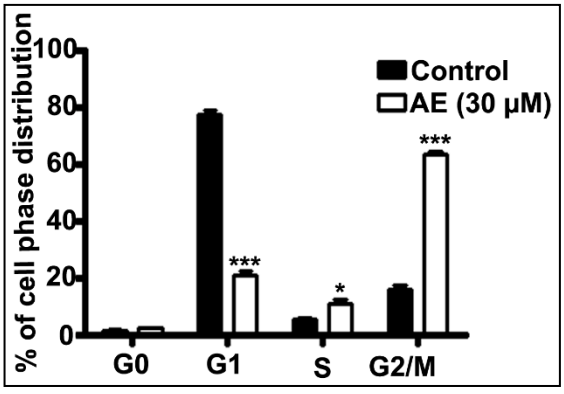

Aloe emodin inhibits cell cycle regulatory proteins, cyclin B1 and p21

We also checked whether aloe emodin induced cell growth inhibition was due to modulation of cell cycle regulatory proteins, cyclin B1, p53 and p21. Cyclin B1, which binds and activates CDK, is expressed predominantly during G2/M phase and helps the cell to cross G2/M check point. Transcriptional activity of cyclin B1 was analyzed by evaluating cyclin B1 promoter activity and also by mRNA analysis. The result shows that cyclin B1 promoter activity was inhibited by over 5 fold when assessed by luciferase assay (Figure 7).

Figure 7. Aloe emodin inhibits cyclin B1 promoter activity

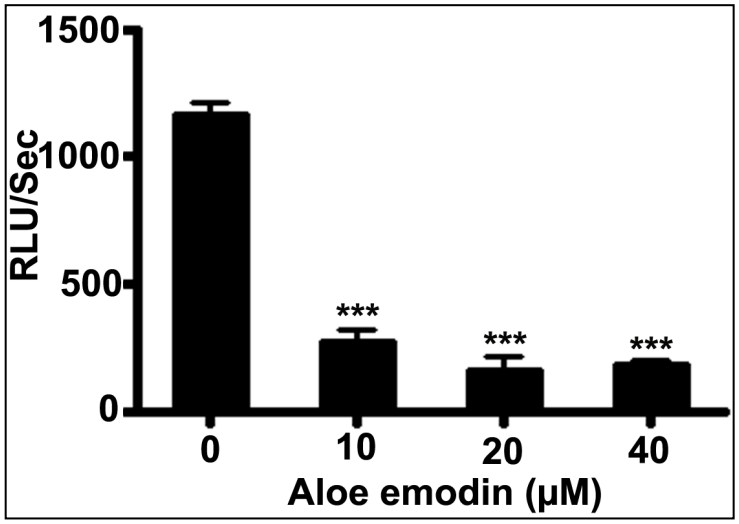

*The cells were transfected with pRL-Null, cyclin B1-Luciferase reporter plasmids using Metafectene. After transfection, the cells were treated with and without aloe emodin and luciferase reporter assays were performed by Dual Luciferase Reporter Assay System following the manufacturer's instruction. The relative luminescence units were normalized for the pRL-Null activity/protein content. Each value is presented as the mean ± SD of determinations from three independent experiments. The mean RLU (Relative Luminescence Unit) of aloe emodin treated samples were significantly lower than the corresponding untreated group as analyzed by One-way ANOVA followed by Tukey's post hoc t- test analysis. ***P < 0.001.*

Cyclins are the proteins which appear at regular intervals during the course of cell division. To identify the time point at which cyclin B1 expresses maximally, we synchronized the cells at G0 stage by serum starvation and isolated the protein at various time points after activating with serum and performed Western blot analysis. Cyclin B1 levels were found to be increased more than 4 fold at 12 h of serum activation and continued to be activated till 24 h (Figure 8, 9).

Figure 8. Increase in cyclin B1 expression after serum activation

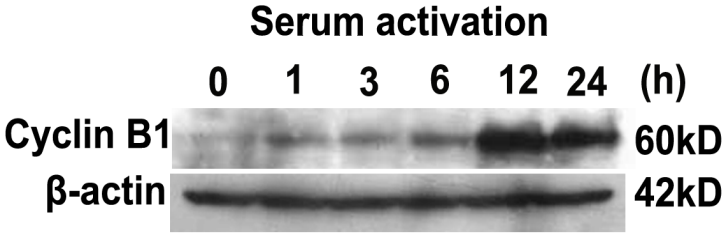

Cells were synchronised at G0 stage by serum starvation. Whole cell lysate was prepared by harvesting the cells at different time points after serum activation. The cell lysates were analyzed for the expression of cyclin B1 by Western blotting.

Figure 9. Fold increase in cyclin B1 expression after serum activation

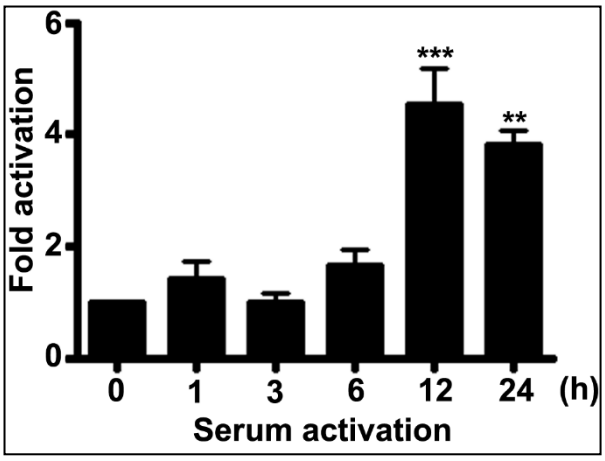

*Fold increase of the cyclin B1 protein expression at various time points after serum activation was normalized with that of β-actin and was plotted as a graph. Each value is presented as the mean ± SD of determinations from two independent experiments. The mean fold change at 12/24 h was significantly higher from the corresponding control group as analyzed by Student's t-test. **P < 0.01; ***P < 0.001.*

We checked for cyclin B1 expression at 12 h with varying concentrations of aloe emodin and a 9 fold decrease was observed for cyclin B1 at 40 µM aloe emodin (Figure 10, 11).

Figure 10. Cyclin B1 expression on treatment with aloe emodin

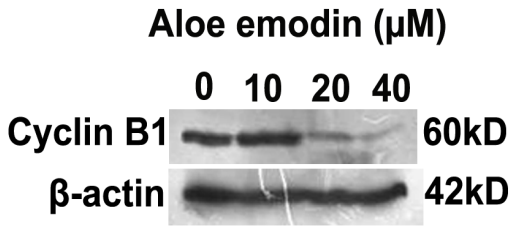

Cells were treated with indicated concentrations of aloe emodin for 12 h. The cell lysates were analyzed for levels of cyclin B1 expression by Western blotting. The above experiments were repeated at least three times.

Figure 11. Fold change of the cyclin B1 protein expression

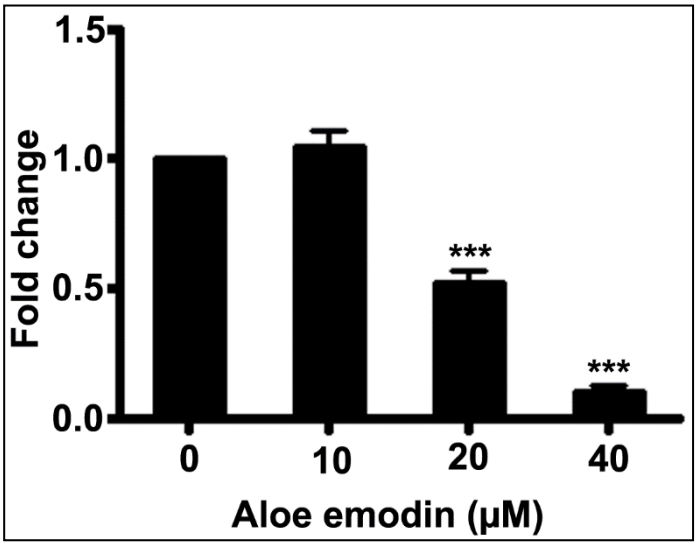

*Fold change of the cyclin B1 protein expression with varying concentrations of aloe emodin was normalized with that of β-actin and was plotted as a graph. Each value is presented as the mean ± SD of determinations from three independent experiments. The mean fold change was significantly lower than the corresponding control group as analyzed by Student's t-test. ***P < 0.001.*

p21 and p53 are the major regulators of cell cycle machinery and to find out whether inhibition of cyclin B1 was mediated by these molecules we analyzed the expression of p21 and p53 at mRNA and protein levels. Results revealed that aloe emodin did not alter the p21 and p53 mRNA levels (Figure 12).

Figure 12. p53/p21 mRNA expression in aloe emodin treated cells

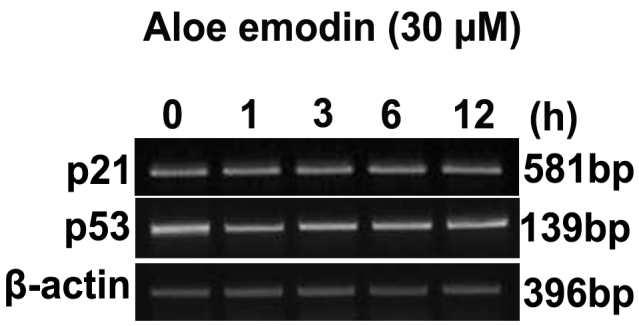

The cells were incubated with 30 μM aloe emodin for indicated time points. After treatment, total RNA was isolated using Pure Link RNA Mini Kit following manufacture's protocol. RNA was reverse transcribed into cDNA and then amplified by using specific primers. The amplified PCR products were electrophoresed on 2% agarose gel and documented.

There was a time dependent increase in p21 protein expression even though the p53 protein levels remained unaltered (Figure 13, 14).

Figure 13. p53/p21 protein expression in aloe emodin treated cells

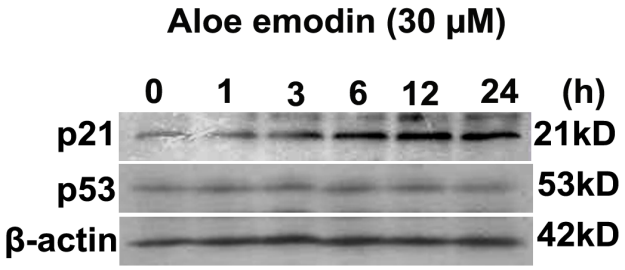

Cells were treated with 30 μM aloe emodin for indicated time points. The cell lysates were evaluated for levels of p53 and p21 by Western blotting. Each experiment was repeated three times.

Aloe emodin was able to activate p21 expression as early as 3 h and to a maximum level of 3.3 fold by 12 h which persisted up to 24 h when compared to control (Figure 14).

Figure 14. Fold change of the p21/p53 protein expression

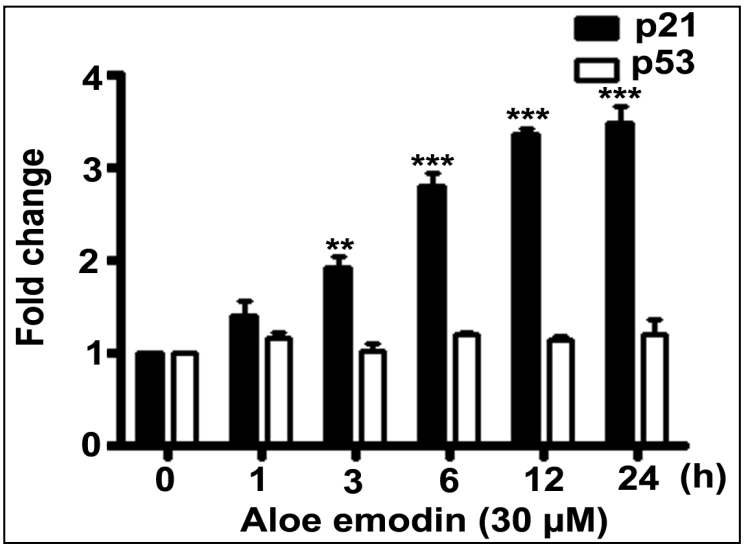

*Fold change of the p21/p53 protein expression at various time points after aloe emodin treatment was normalized with that of β-actin and was plotted as a graph. Each value is presented as the mean ± SD of determinations from three independent experiments. The mean fold change was significantly higher than the corresponding control group as analyzed by Student's t-test. **P < 0.01; ***P < 0.001.*

Overall these results indicate that aloe emodin inhibits tumor cell proliferation and exerts growth inhibitory actions through alterations of cell cycle and cell cycle regulatory proteins p21 and cyclin B1.

B. Apoptosis induction ability of aloe emodin

Apoptosis is the process of programmed cell death characterised by changes including cell shrinkage, chromatin condensation, chromosomal DNA fragmentation and membrane blebbing. It was originally believed that cancer is associated with accumulation of cells due to an increase in cellular proliferation, but is now known that it is also due to a decrease in cell death. Apoptosis induction ability is the one of the basic requisite for a compound to be considered as having anticancer potentials. Morphological observations revealed the apoptotic potential of aloe emodin by externalization of phosphatidyl serine present on the plasma membrane and loss of mitochondrial membrane integrity, DNA fragmentation etc. On treatment with AE we observed positive annexin staining, loss of mitochondrial membrane potential and strong TUNEL positivity. Apart from these apoptosis specific morphological changes, molecular analysis also revealed the apoptosis induction ability of aloe emodin as it

activated caspases 9/6 and inactivated PARP. Aloe emodin induced apoptotic execution in WiDr cell was found to be solely dependent on the caspase 6 since caspase 3 and caspase 7 were not activated on treatment.

Externalization of phosphatidylserine by aloe emodin

A critical stage of apoptosis involves the acquisition of surface changes by dying cells that eventually results in the recognition and the uptake of these cells by phagocytes. Externalization of phosphatidylserine (PS) is one such phenomenon that has been extensively studied. PS is predominantly observed on the inner surface of the plasma membrane facing the cytosol. When externalized, annexin binds with PS and bright green annexin FITC staining was imparted to membrane of the aloe emodin treated cells, confirming the presence of phosphatidylserine on the outer cell membrane, a sign of early stages of apoptosis (Figure 15).

Figure 15. Annexin binding of cells induced by aloe emodin

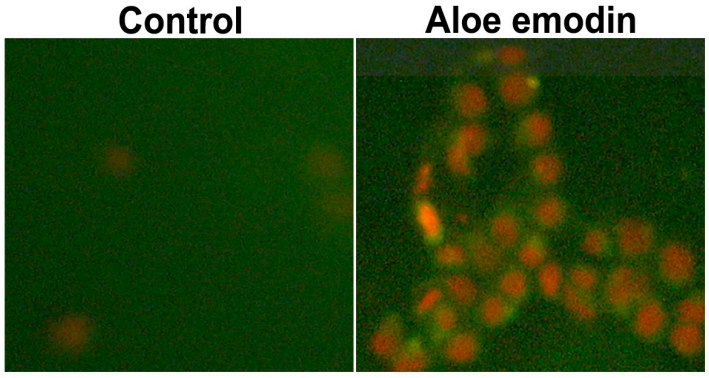

Cells were treated with or without aloe emodin (conc for 16 h and were stained with annexin-fluorescein isothiocyanate/propidium iodide mixture using an apoptosis detection kit as per the manufacturer's protocol. The cells were viewed under an inverted fluorescent microscope and photographed. These results were confirmed in another independent experiment.

Loss of mitochondrial membrane potential by aloe emodin

The mitochondrial membrane permeability transition is an important characteristic of cells undergoing apoptotic death. Mitosensor is a lipophilic, cationic dye that can selectively enter

into mitochondria and reversibly change color from green to red as the membrane potential increases. In healthy cells with high mitochondrial membrane potential (ΔΨm), Mitosensor spontaneously forms complexes known as J-aggregates with intense red fluorescence. On the other hand, in apoptotic or unhealthy cells with low ΔΨm, Mitosensor remains in the monomeric form, which shows only green fluorescence. Reduction in the mitochondrial membrane potential of aloe emodin treated cells shown by green fluorescence shows apoptosis induction ability of aloe emodin (Figure 16).

Figure 16. Changes in mitochondrial membrane potential (ΔΨm) induced by aloe emodin

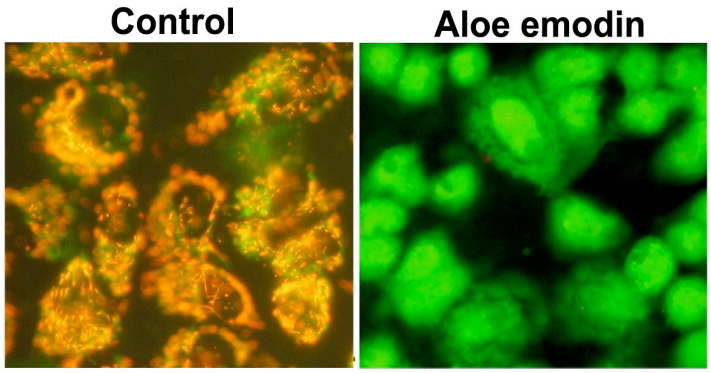

Cells were treated with or without aloe emodin for 12 h and stained with Mitosenor. The cells were viewed under an inverted fluorescent microscope and photographed. These results were confirmed in another independent experiment.

DNA fragmentation induced by aloe emodin

Terminal Transferase dUTP Nick End Labeling (TUNEL) Assay is a method used to detect DNA degradation in apoptotic cells because one of the hallmarks of late stage apoptosis is the fragmentation of nuclear chromatin which results in a multitude of 3'-hydroxyl termini of DNA ends. This property can be used to identify apoptotic cells by labeling the DNA breaks with FITC-tagged deoxyuridine triphosphate nucleotides (FITC-dUTP). The enzyme terminal deoxynucleotidyl transferase (TdT) catalyzes a template-independent addition of deoxyribonucleoside triphosphates to the 3'- hydroxyl ends of double- or single-stranded DNA strands with exposed 3'-hydroxyl ends. Once incorporated into the DNA, FITC can be detected by an anti-FITC antibody using standard immunohistochemical techniques. Non-apoptotic cells do not incorporate much of the FITC-dUTP because of absence of exposed 3'-hydroxyl DNA ends. An extensive DNA break shown by strong TUNEL positive cells on treatment supports apoptosis induction ability of aloe emodin (Figure 17).

Figure 17. DNA fragmentation in cells induced by aloe emodin

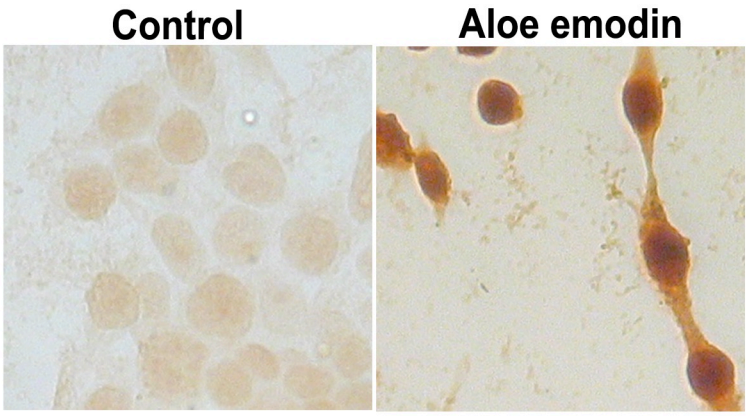

Cells were treated with or without aloe emodin for 24 h and free OH- end produced by DNA fragmentation was labelled with FITC conjugated dUTP using an in situ cell death detection kit as per manufacturer's protocol. The cells were viewed under an inverted bright field microscope and photographed. These results were confirmed in another independent experiment.

Activation of caspases by aloe emodin

Determination of pro and cleaved caspases by aloe emodin

Caspases are a family of proteases that are one of the main executors of apoptotic process. They belong to a group of enzymes known as cysteine proteases and exist within the cell as inactive pro-forms or zymogens. These zymogens can be cleaved to form active enzymes following the induction of apoptosis. Induction of apoptosis results in the activation of initiator caspase such as caspase -8, -9, -10 etc. These caspases can then activate effector caspases, such as caspase -3, -6 and -7. These caspases are responsible for the cleavage of the key cellular proteins, such as cytoskeletal proteins and PARP that leads to the typical morphological and biochemical changes observed in cells undergoing apoptosis. The mitochondria are key regulators of the caspase cascade and apoptosis. Loss in mitochondrial membrane potential leads to the release of cytochrome C from mitochondria that can result in the activation of caspase -9, and then subsequent effector caspases. We analyzed the role of initiator caspase -9 and effector caspases -3, -6, and -7 in the aloe emodin induced apoptotic cell death. Among the four caspases analyzed we observed activation in caspase -9 and -6 only. Activation of caspases was initially determined by the expression levels of procaspase -6/ -9 upon treatment with aloe emodin in a

time dependent manner. This was further confirmed by assessing concomitant levels of cleaved fragments of caspases -6 and -9 (Figure 18, 19).

Figure 18. Caspase -9 expression in aloe emodin treated cells

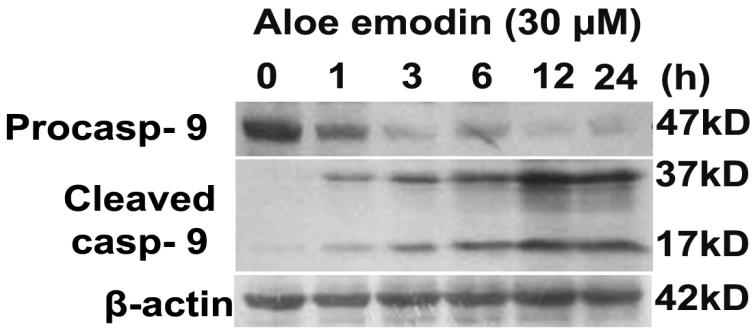

Cells were treated with 30 μM of aloe emodin for indicated time points. The cell lysates were evaluated for levels of respective procaspase -9/cleaved caspase -9 expression by Western blotting. The above experiment was repeated at least three times.

Figure 19. Caspase -6 expression in aloe emodin treated cells

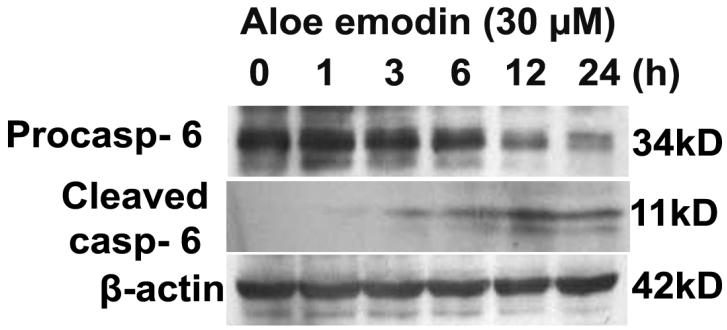

Cells were treated with 30 μM of aloe emodin for indicated time points. The cell lysates were evaluated for levels of respective procaspase -6/cleaved caspase -6 expression by Western blotting. The above experiment was repeated three times.

It is evident that procaspse -9 was decreased by 10 fold compared to the untreated control while the decrease in procaspase -6 was nearly 2.9 fold (Figure 20).

Figure 20. Fold change of procaspase -9/6 in aloe emodin treated cells

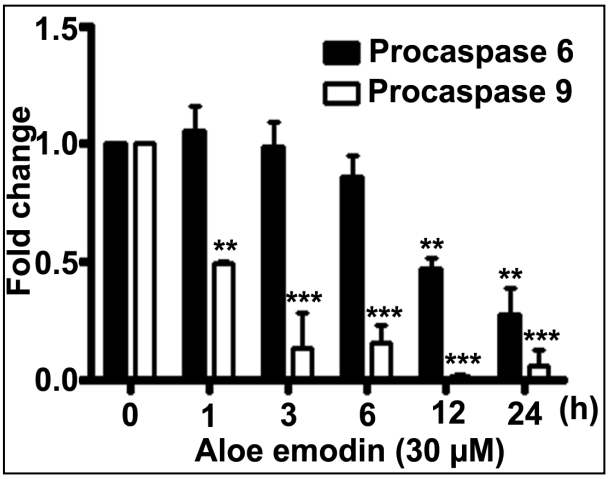

*Fold change of the procaspase -9/procaspase -6 proteins at various time points after aloe emodin treatment was normalized with that of β-actin and was plotted as a graph. Each value is presented as the mean ± SD of determinations from three independent experiments. The mean fold change was significantly lower than the corresponding control group as analyzed by Student's t-test. *P < 0.05; **P < 0.01; ***P < 0.001.*

On analysis of the increase in cleaved caspase -9, we observed 12 fold increase compared to the untreated control, whereas the increase in cleaved caspase -6 was 4 fold (Figure 21).

Figure 21. Fold change of cleaved caspase -9/6 in aloe emodin treated cells

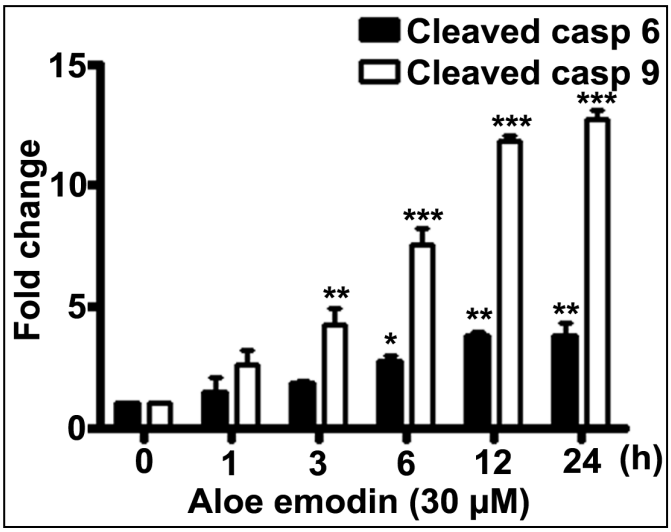

*Fold change of the cleaved caspase -9/caspase -6 proteins at various time points after aloe emodin treatment was normalized with that of β-actin and was plotted as a graph. Each value is presented as the mean ± SD of determinations from three independent experiments. The mean fold change was significantly higher than the corresponding control group as analyzed by Student's t-test. **P < 0.01; ***P < 0.001.*

Caspase -3 has been identified as being a key mediator of apoptosis of mammalian cells. Caspase -7 is also an executioner protein of apoptosis. The expression of caspase -3 and -7 remain unaltered upon treatment with aloe emodin (Figure 22, 23).

Figure 22. Caspase -3 expression in aloe emodin treated cells

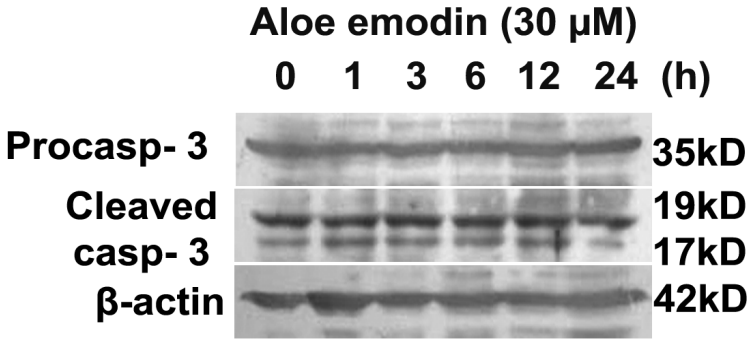

Cells were treated with 30 μM of aloe emodin for indicated time points. The cell lysates were evaluated for levels of respective procaspase -3/cleaved caspase -3 expression by Western blotting. The above experiment was repeated at least three times.

Figure 23. Caspase -7 expression in aloe emodin treated cells

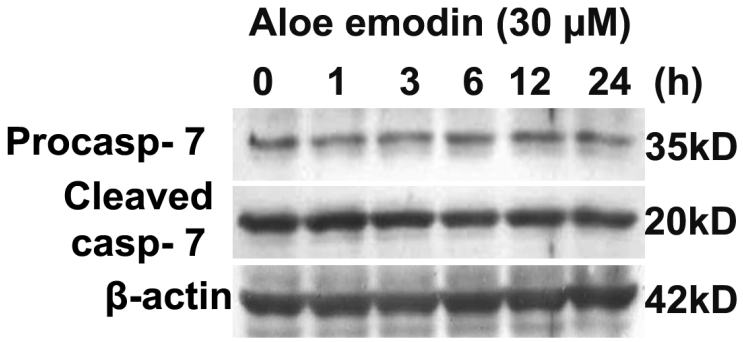

Cells were treated with 30 μM of aloe emodin for indicated time points. The cell lysates were evaluated for levels of respective procaspase -7/cleaved caspase -7 expression by Western blotting. The above experiment was repeated at least three times.

To understand whether this is a WiDr cell specific action, we used a known caspase -3 inducing compound, curcumin. We observed 2 fold activation of caspase -3 after treatment of curcumin (25 µM) for 24 h at the same time aloe emodin (30 µM) was unable to activate caspase -3 (Figure 24, 25).

Figure 24. Caspase -3 expression in curcumin treated cells.

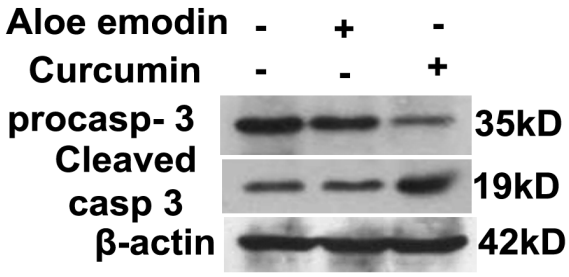

Cells were treated with 30 µM of aloe emodin/25 µM curcumin for 24 h. The cell lysates were evaluated for levels of procaspase -3/cleaved caspase -3 by Western blotting. The experiment was repeated another time with similar results.

Figure 25. Fold change of caspase -3 in curcumin treated cells

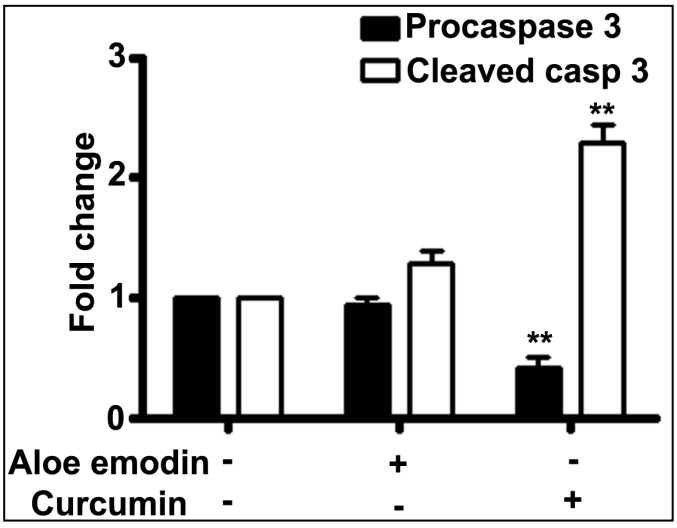

Fold change of the procaspase -3/cleaved caspase -3 protein after curcumin treatment was normalized with that of β-actin and was plotted as a graph. Each value is presented as the mean ± SD of determinations from three independent experiments. The mean fold change was

*significantly different from the corresponding control group as analyzed by Student's t-test. **P < 0.01.*

Determination of aloe emodin induced caspase activity

Since caspases are functional enzymes, the critical method for the analysis of its regulation is by determination of its activity. Accurate determination of caspase activity was made by analysing caspase -3/7 and -9 by luminometry and caspase -6 by fluorometry. Caspase -3/7 assay was also found supporting the above results showing no change after 48 h treatment with 30 µM aloe emodin, whereas 50 µM tamoxifen for 2 h resulted in 2 fold increase in caspase-3/7 activity (data not shown). Caspase -9 and caspase -6 assay showed 8.7 and 5.9 fold activation on treatment with 40 µM of aloe emodin for 48 h and 24 h respectively (Figure 26, 27).

Figure 26. Activity of Caspase -3/7 and -9 in aloe emodin treated cells

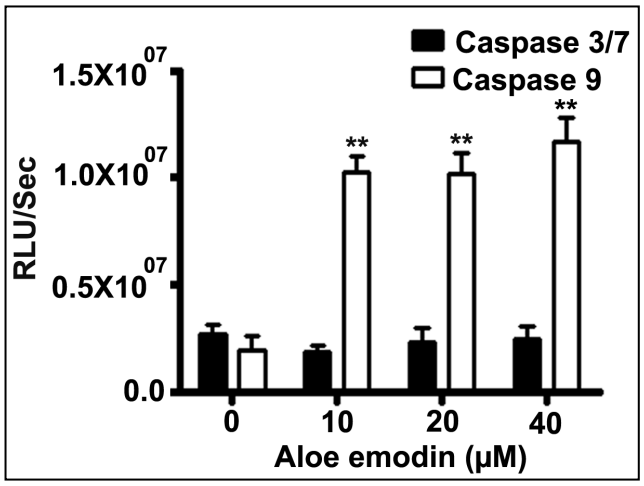

*Cells were treated with indicated concentrations of aloe emodin for 48 h. After treatment, cells were lysed and caspase activities were determined. The experiments were repeated another time with similar result and the caspase activities were expressed as fold activation over the untreated control. The mean change in RLU of aloe emodin treated samples were compared with the untreated control sample and analyzed by One-way ANOVA followed by Tukey's post hoc t- test analysis. **P < 0.01.*

Figure 27. Activity of caspase -6 in aloe emodin treated cells

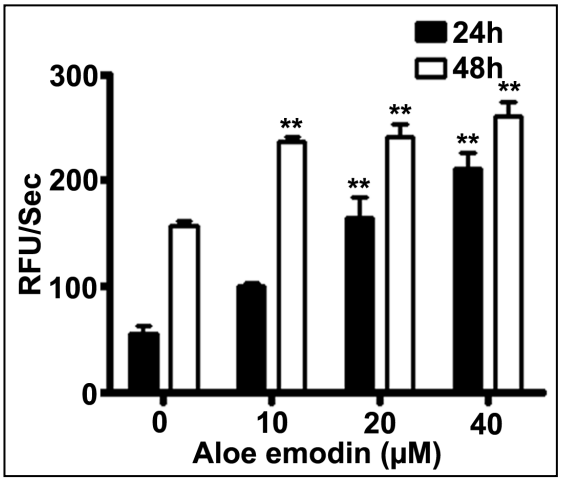

*Cells were treated with indicated concentrations of aloe emodin for 24/48 h. After treatment, cells were lysed and caspase-6 activity was determined. The experiments were repeated another time with similar result and the caspase activity was expressed as fold activation over the untreated control. The mean change in RFU (Relative Fluorescence Unit) of aloe emodin treated sample was significantly higher when compared with the untreated control sample as analyzed by One-way ANOVA followed by Tukey's post hoc t- test analysis. **P < 0.01.*

Cleavage of PARP by aloe emodin

The cleavage of DNA repair associated nuclear enzyme PARP to form an 89 kD fragment has become a hallmark for apoptosis in most types of cells. The detection of cleaved PARP is a very sensitive marker for the detection of apoptosis. Cleaved PARP correspond to the actions of the executioner caspases. Caspase -3, -6 and -7 are considered as apoptotic executioner caspases. Aloe emodin (30 μM) specifically activated executioner caspase- 6 which facilitated the cleavage of PARP in a time dependent manner. We observed persistent 2.7 fold increase in fragment of PARP from 3 h onwards on treatment of aloe emodin (Figure 28, 29).

Figure 28. Cleavage of PARP in aloe emodin treated cells

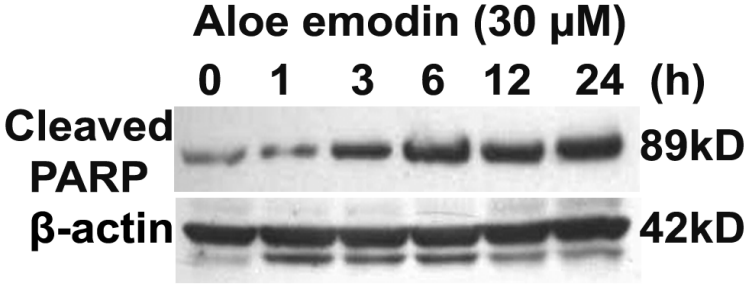

Cells were treated with 30 μM of aloe emodin for indicated time points. The cell lysates were evaluated for levels of cleaved PARP expression by Western blotting. The above experiment was repeated at least three times.

Figure 29. Fold change of cleaved PARP in aloe emodin treated cells

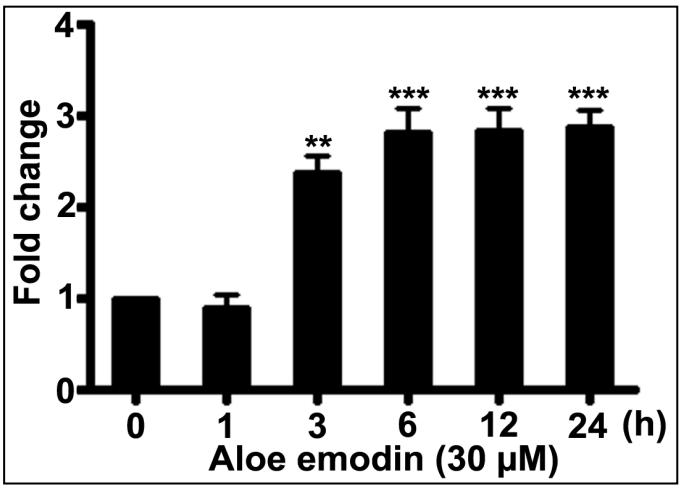

*Fold change of the cleaved PARP protein at various time points after aloe emodin treatment was normalized with that of β-actin and was plotted as a graph. Each value is presented as the mean ± SD of determinations from three independent experiments. The mean fold change was significantly higher than the corresponding control group as analyzed by Student's t-test. **P < 0.01; ***P < 0.001.*

Involvement of MAPK signalling in aloe emodin induced antiproliferative and apoptotic effect

To evaluate the effect of aloe emodin on intracellular signal transduction, we examined the levels of phosphorylated ERK1/2, SAPK/JNK1/2, p38 MAPK in cells using western blot. Extra cellular signal regulated kinases are important candidate of proteins which assist cell division and proliferation. To determine whether ERK signalling is involved in aloe emodin induced antiproliferative effect in WiDr cells, the lysates from the cells treated with aloe emodin were immunoblotted for the activated forms of ERK1/2 with an antibody specific for phosphorylated ERK1/2 (Thr202 and Tyr204). Levels of phosphorylated ERK were downregulated in aloe emodin treated cells by about 2.2 fold. These results demonstrate that signalling through ERK is necessary for aloe emodin to exert its antiproliferative effect (Figure 30, 31).

Figure 30. Expression of phosphoMAPKs in aloe emodin treated cells

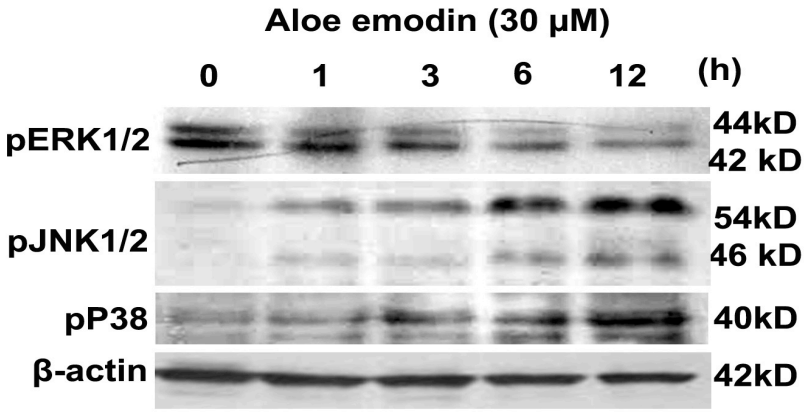

Cells were treated with 30 μM of aloe emodin for indicated time points. The cell lysates were evaluated for levels of pERK1/2, pP38, pJNK1/2 expression by Western blotting.

Activation of SAPK/JNK occurs through phosphorylation of threonine183 and tyrosine 185. Dually phosphorylated active dimer of SAPK/JNK can translocate to the nucleus where it regulates transcription through its effect on c-jun and other transcription factors. Activated p38 MAPK by phosphorylation (Thr180/Tyr182) can activate various other kinases and transcription factors. Aloe emodin (30 μM) amplified phosphorylation of p38 and SAPK/JNK at their corresponding threonine and tyrosine residues by about 2.2 fold in both cases (Figure 30, 31).

Figure 31. Fold change of MAPKs in aloe emodin treated cells

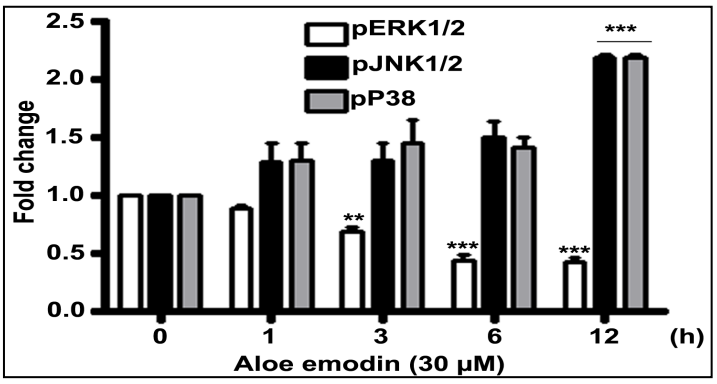

*Fold chnage was normalized with that of β-actin and was plotted as a graph. Each value is presented as the mean ± SD of determinations from three independent experiments. The mean fold change was significantly different from the corresponding untreated group as analyzed by One-way ANOVA followed by Tukey's post hoc t- test analysis. *P < 0.05; **P < 0.01; ***P < 0.001.*

Our results supported that both JNK and p38 were activated during aloe emodin treatment. In such case, inhibition of these kinases should bring down the apoptotic effect induced by aloe emodin. In an attempt to establish the role of MAPKs in aloe emodin induced antiproliferative effect we evaluated viability after treatment with MAPK inhibitors/aloe emodin. We used inhibitors for JNK and p38 (SP600125 and SB203580) since we observed activation in both MAPKs upon treatment with aloe emodin. Results showed that both inhibitors imparted a protective effect over the antiproliferative activity of aloe emodin eventhough the levels of protection was differed (Figure 32).

Figure 32. Effect of JNK/p38 inhibitors on viability of aloe emodin treated cells

*Cells were treated with 10 μM of each inhibitor for 12 h prior to the treatment with aloe emodin for 48 h. At the end of treatment, cell viability was assessed by MTT assay. All results were expressed as the mean percentage of control ± S.D. of quadruplicate determinations from three independent experiments. The differences among the mean values were analyzed using One-way ANOVA followed by Tukey's post hoc t- test analysis. The One-way ANOVA revealed that the average mean values of cell survival differed significantly in control versus aloe emodin/inhibitors treated cells. *P < 0.05; **P < 0.01.*

In summary, aloe emodin activated cell death by apoptosis by downregulating the phosphorylation of extra cellular signal regulated kinase1/2 and at the same time activating SAPK/JNK and p38 MAPK. The latter signals direct the cells to apoptosis. Aloe emodin

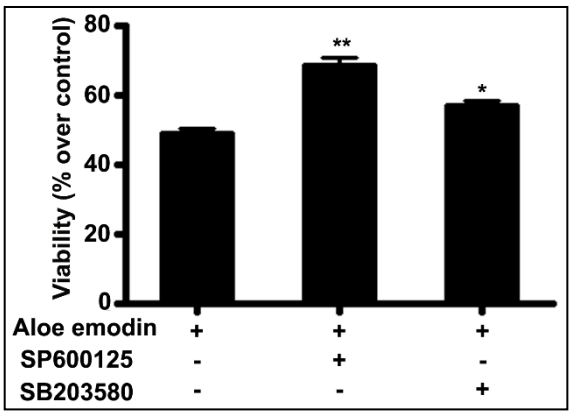

induced cell death was through mitochondrial pathway by activating initiator caspase -9 and subsequent activation of effector caspase -6.

C) Inhibition of cell migration/invasion by aloe emodin

Cell migration, the movement of cells from one area to another is a central event in metastasis of tumors. Cell invasion is similar to cell migration; however, it requires a cell to migrate through an extracellular matrix (ECM) or basement membrane extract (BME) barrier by first enzymatically degrading the barrier in order to become established in a new location. Learning more about the cellular and molecular basis of migration/invasion programmes will help us to understand how cancer cells disseminate and lead to new treatment strategies. Our results showed that a relatively non toxic level of aloe emodin suppressed the phorbol-12-myristyl-13-acetate (PMA) induced migration and invasion. On analysis of the molecules involved in the migration and invasion, we found mRNA expression of MMP-2, 9 and RhoB were downregulated.

Aloe emodin prevents *in vitro* cell migration

Aloe emodin inhibits migration of cells into wounded area

All experiments for anti-migratory effect of aloe emodin were carried out in presence of PMA (100 ng/ml). PMA is a potent tumor promoter often employed in biomedical research to activate various signalling molecules. It binds and activates protein kinase C, which is an enzyme that controls the function of other proteins. This property gives phorbols the capacity to act as tumor promoters. Inhibitory effect of aloe emodin on colon cancer cell migration was evaluated by scratch wound migration assay. A concentration of 20 μM aloe emodin for 24 h effectively reduced the PMA induced migration of cells in to the wounded area, which was determined as distance moved by cells (in μm) into the wound (Figure 33).

Figure 33. Analysis of cell migration of aloe emodin treated cells

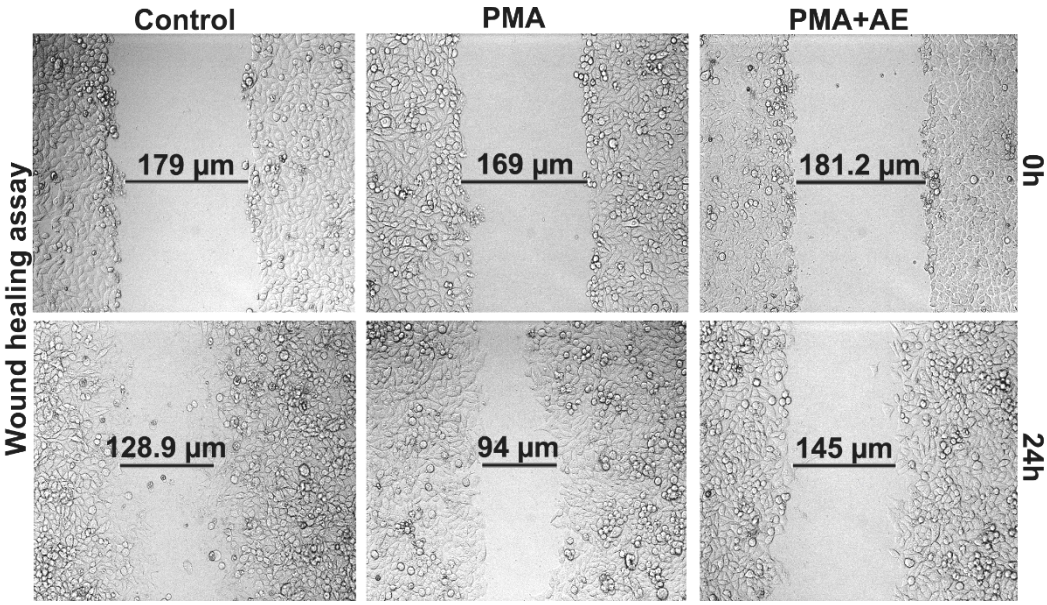

Cells were allowed to migrate into a wounded area with and without PMA/aloe emodin. Cell migration into the wound surface was then monitored by microscopy after 24 h and reported as the width of remaining wounded area relative to the initial wound area.

PMA-induced migration was inhibited by 2 fold after treatment with aloe emodin (Figure 34).

Figure 34. Graphical representation of scratch wound assay

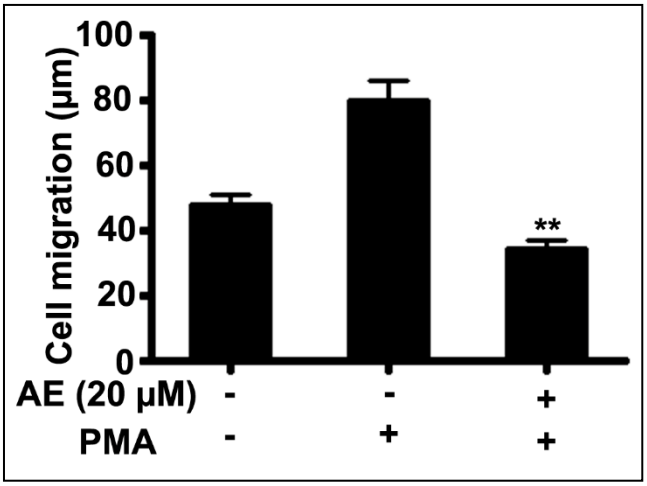

The assay was independently repeated three times and the values are plotted as graph. The mean distance migrated by cells was significantly lower in the aloe emodin treated sample as

*analyzed using One-way ANOVA followed by Tukey's post hoc t- test analysis. Bars indicate S.D. **P < 0.01.*

Aloe emodin inhibits transwell migration/invasion

Inhibitory effect of aloe emodin (20 µM) on colon cancer cell migration/invasion was evaluated by a modified Boyden's chamber. The influence of aloe emodin on migration through a membrane of 8 µm pore was examined in WiDr colon cancer cells. Here also we used PMA as an inducer of cell migration (Figure 35).

Figure 35. Inhibition of transwell migration of cells by aloe emodin

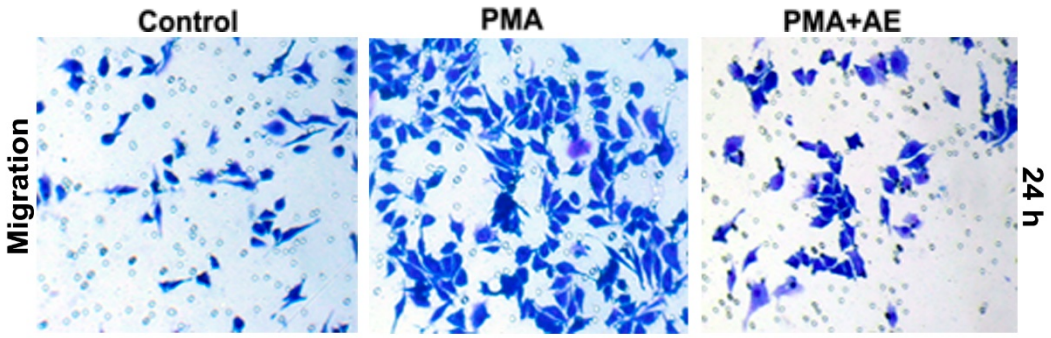

Migration of cells was determined with modified Boyden's chamber method. Response of cells for aloe emodin was assayed using 24-well migration chamber with an upper well having a membrane of 8 µm pore and 12 mm of diameter. Cells on the upper side of the membrane were carefully removed by using a wet cotton swab after incubation with aloe emodin/PMA and migrated cells were stained with crystal violet and counted.

We then evaluated for the anti-invasive property of aloe emodin. To analyze the anti-invasive property of aloe emodin we used culture inserts coated with Matrigel. Matrigel is a solubilized basement membrane preparation extracted from EHS mouse sarcoma, a tumor rich in ECM proteins. Its major component is laminin, followed by collagen IV, heparan sulfate proteoglycans, and entactin 1. At room temperature, Matrigel polymerizes to produce biologically active matrix material resembling the mammalian cellular basement membrane. Cells behave as they do in vivo when they are cultured on Matrigel. It provides a physiologically relevant environment to study invasion. PMA treated cells showed increased invasiveness when compared to cells treated with control medium alone. Aloe emodin

successfully diminished the number of cells invaded through the basement membrane matrix coated culture inserts (Figure 36).

Figure 36. Inhibition of transwell invasion of cells by aloe emodin

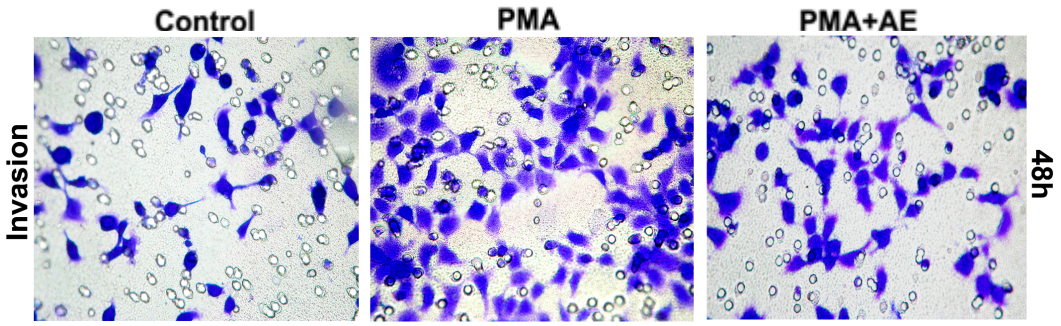

Invasion of cells was determined with modified Boyden's chamber method. In case of assessing cell invasion BioCoat Martigel Invasion Chambers were used. Response of cells for aloe emodin was assayed using 24-well migration chamber with an upper well having a membrane of 8 µm pore coated with Matrigel. Cells on the upper side of the membrane were carefully removed by using a wet cotton swab after incubation with aloe emodin/PMA and migrated cells were stained with crystal violet and counted.

A graphical representation of inhibition of transwell migration/invasion is given in Figure 37. Treatment with aloe emodin reduced the PMA induced transwell migration and invasion of cells by over 1.5 and 3.5 fold respectively.

Figure 37. Number of cells migrated/invaded

The experiment was repeated three times with similar results and the number of cells migrated/invaded was counted and plotted in the graph. The mean number of cells migrated/invaded was significantly lower in the aloe emodin treated sample as analyzed by

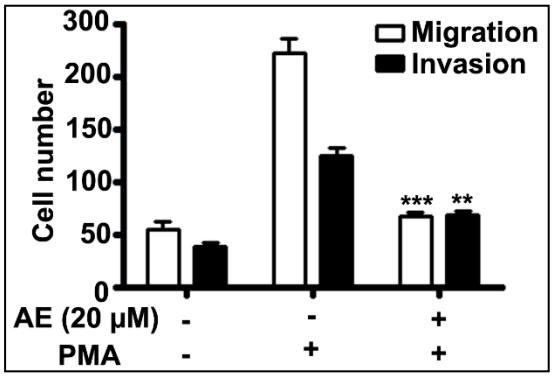

*One-way ANOVA followed by Tukey's post hoc t- test analysis. Bars indicate S.D. **P < 0.01; ***P< 0.001.*

These results provided clue regarding involvement of various molecular targets in aloe emodin mediated inhibition of migration/invasion and prompted us to evaluate the prominent MMPs and Rho family proteins involved in cell migration/invasion.

Aloe emodin inhibits PMA induced expression of MMPs and RhoB

Cellular movements are enhanced by the degradation of extra cellular components by activating a set of genes called matrix metalloproteinases. These proteinases are capable of degrading all kinds of extracellular matrix proteins and carve the way for cancer cell to tread distant sites. RhoB comes under the Rho family of proteins which aid in cell movement by giving flexibility to cell through cytoskeletal reorganization. An effective way to control tumor cell growth is by controlling the spread of tumor cells from one site to another. In this study we evaluated whether aloe emodin could regulate the expression of MMPs that are found to be activated in various malignant tumors. For these experiments, we used PMA which is known to induce MMPs/Rho protein expression in cancer cells.

Aloe emodin inhibits PMA induced MMP-2/9 mRNA expression

Semiquantitive RT-PCR analysis of MMPs genes showed that aloe emodin could effectively inhibit MMP -2, -7, -9, -14 and -15 although to different extent (Figure 38).

Figure 38. SQRT-PCR analysis of MMPs/TIMPs in aloe emodin treated cells

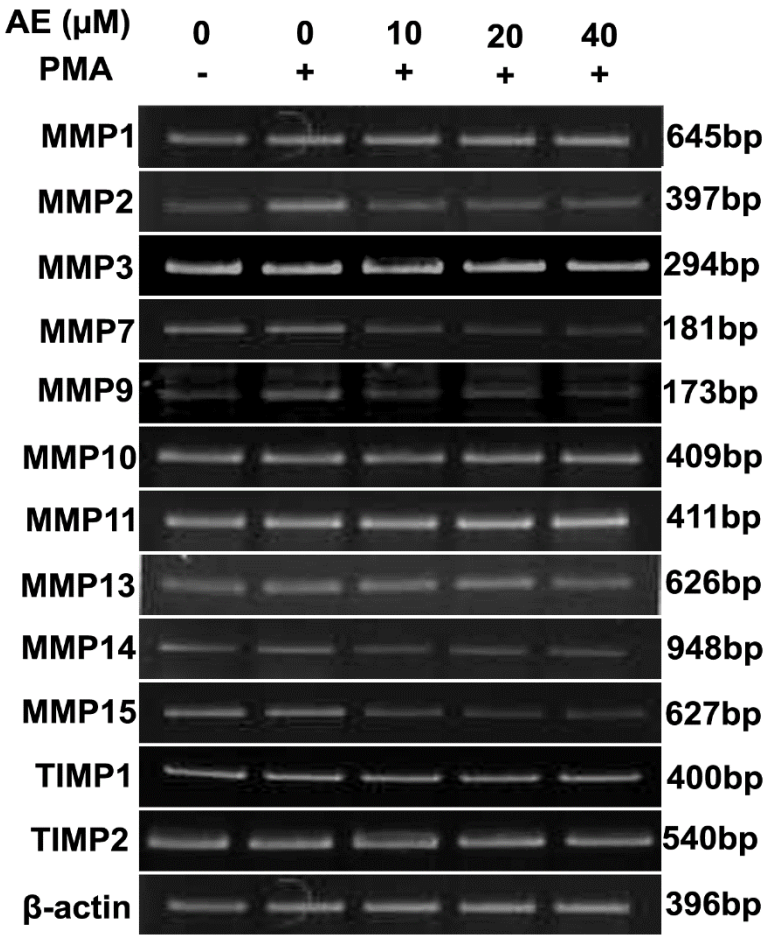

RNA was isolated and reverse transcribed into cDNA and then amplified by using specific primers. The amplified PCR products were electrophoresed on 2% agarose gel and documented.

We have also analyzed the regulation of MMP -1/-2 by Tissue Inhibitor of Metalloproteinases (TIMPs), aloe emodin was found to be having no effect on the mRNA expression of TIMP -1/-2 (Figure 38). PMA stimulated the expression of MMP-2/9 in WiDr cells whereas MMP-7, -14, and -15 are unaffected on treatment with PMA (Figure 39).

Figure 39. Fold change of MMPs by SQRT- PCR analysis

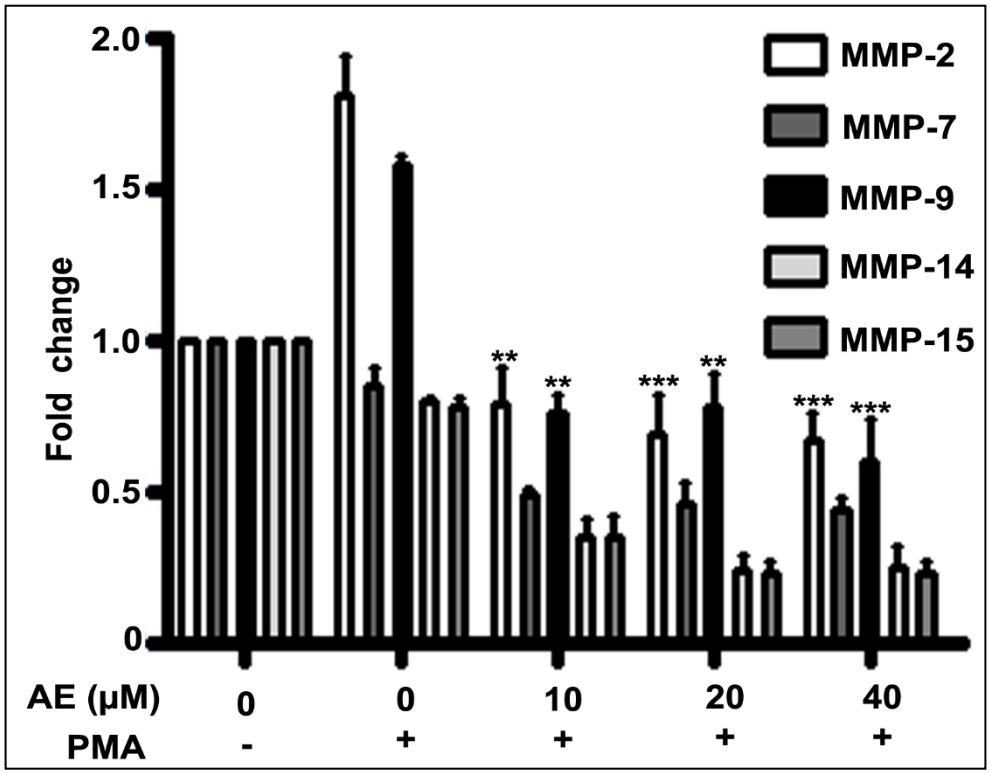

*Fold change of the target mRNAs were normalized with that of β-actin and is plotted as a graph. Each value is presented as the mean ± SD of determinations from two independent experiments. The mean fold change was significantly lower than the corresponding PMA treated group as analyzed by Student's t-test. **P < 0.01; ***P < 0.001.*

Inhibition of PMA induced MMP -2/9 mRNA expression by aloe emodin was subsequently validated by Real Time RT-PCR. The decrease in the expression of MMP-2/9 in aloe emodin treated cells were nearly 2 and 3 folds respectively (Figure 40).

Figure 40. Real Time RT-PCR analysis of MMP-2/9 inhibition by aloe emodin

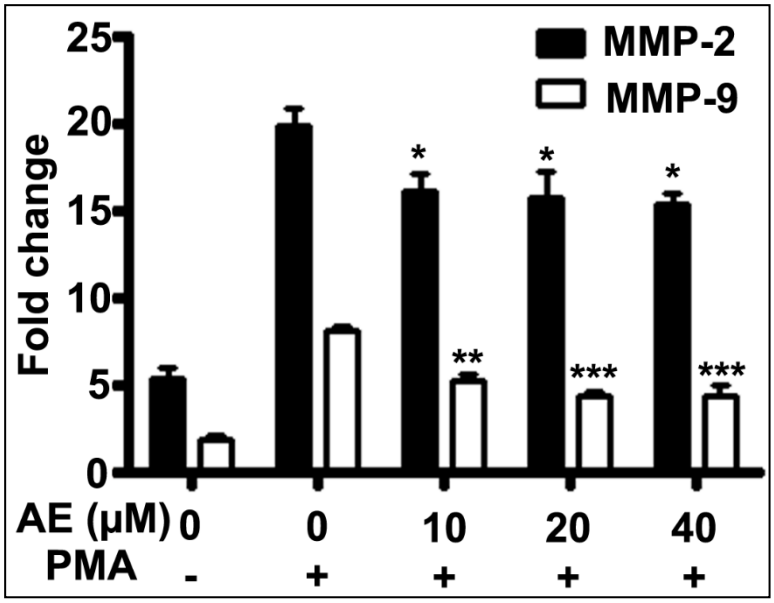

*The real- time PCR was performed by 1 μg of cDNA and 2 pmol primers per reaction in 7900 HT Fast Real- Time PCR system using MESA green qPCR Mastermix for SYBR Assay. Fold change of the target mRNAs were normalized with that of β-actin and is plotted as a graph. Each value is presented as the mean ± SD of determinations from two independent experiments. The mean fold change was significantly lower than the corresponding PMA treated group as analyzed using One-way ANOVA followed by Tukey's post hoc t- test analysis. **P < 0.01; ***P< 0.001.*

Aloe emodin hinders MMP-2/9 promoter activity

To conform the mode of downregulation of PMA induced MMP-2/9 mRNA level, we performed a promoter activity assay. The effects of aloe emodin on PMA induced MMP-2 promoter activity was investigated by luciferase reporter gene assay using the amplified 1584 bp fragment that was cloned into pGL3 basic vector (pGL3-MMP-2-luc). This promoter portion bears multiple binding sites for transcription factors including NF-κB, CREB, and AP-1 (Lee et al., 2008). MMP-9 promoter activity was investigated by luciferase reporter gene assay using a proximal 0.67 kb fragment of the human MMP-9 promoter inserted into pGL3 basic vector (pGL3-MMP-9-luc). This promoter portion also bears multiple binding sites for transcription factors including NF-κB, Sp-1, and AP-1 sufficient for an optimal induction of MMP-9 promoter activity by cytokines (Gum et al., 1996). Basal activity of MMP-9 promoter was found to be relatively lower when compared to that of MMP-2, but the fold activation of

MMP-9 on treatment with PMA was much higher which accounts around 12.3 fold compared to 2.2 fold in MMP-2. The activation of MMP-2 was subsequently reduced to the basal levels on incubation with aloe emodin (20 µM), whereas the activation of MMP-9 was brought down by 2.8 fold on treatment with aloe emodin (Figure 41, 42).

Figure 41. Aloe emodin inhibits MMP-2 promoter activity

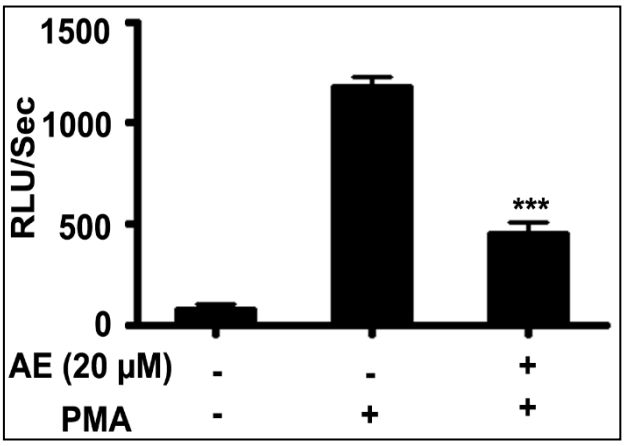

Figure 42. Aloe emodin inhibits MMP-9 promoter activity

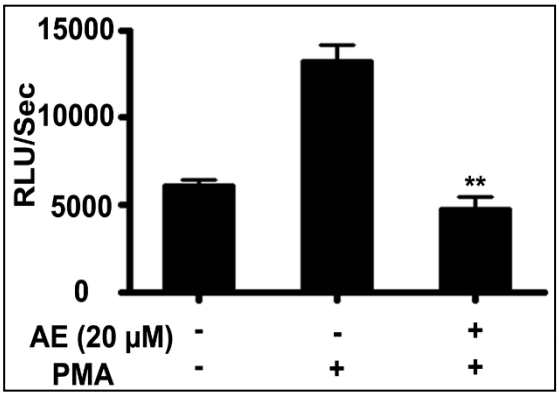

*(Figure 41, 42) The cells were transfected with pRL-Null, MMP-2/MMP-9 luciferase reporter plasmids and treated with and without aloe emodin/PMA. Luciferase reporter assays were performed by Dual Luciferase Reporter Assay System following the manufacturer's instruction. The relative luminescence units were normalized with the pRL-Null activity/protein content. Each value is presented as the mean ± SD of determinations from three independent experiments. The mean RLU of aloe emodin treated sample was significantly lower than the corresponding PMA treated group as analyzed using One-way ANOVA followed by Tukey's post hoc t- test analysis. **P < 0.01; ***P < 0.001.*

Aloe emodin inhibits MMP-2/9 enzymatic activity

We examined whether the reduction in the intracellular MMP-2/9 mRNA content leads to a reduction in MMP-2/9 activity in the culture supernatant. To this end, conditioned media were tested by an MMP-2/9 specific activity assay. Similar to the results obtained by RT-PCR, the PMA-induced MMP-2/9 activity was reduced on co-incubation with 20 µM aloe emodin. PMA treatment induced more than 4.5 fold increase in the MMP-2/9 activity and treatment with aloe emodin diminished the activity to that of unstimulated control cells (Figure 43). This clearly shows that aloe emodin decreases the activity of MMP-2/9.

Figure 43. Inhibition of MMP-2/9 activity by aloe emodin

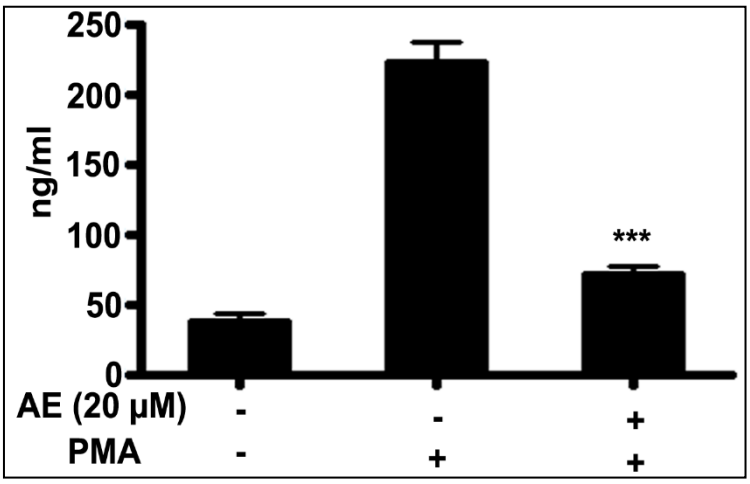

*Gelatinolytic activity was analyzed by using Innozyme Gelatinase MMP-2/9 Activity Assay Kit following the manufacturer's protocol. Each value is presented as the mean ± SD of determinations from three independent experiments. The mean fold change was significantly lower than the corresponding PMA treated group as analyzed using One-way ANOVA followed by Tukey's post hoc t- test analysis. ***P < 0.001.*

Aloe emodin inhibits gelatinolytic activity of culture supernatant

Gelatin zymography is the most commonly used assay for demonstrating the activity of gelatin-degrading proteases, MMP-2/9. We evaluated the effects of aloe emodin on extracellular MMP-2/9 functional activity in WiDr cells treated with PMA, by gelatin-zymography. Cells showed secretion of the two distinct 72 and 92-kD type IV collagenases, MMP-2 and MMP-9 respectively, whose activities were stimulated by PMA. In contrast to MMP-9 levels, a high basal content of MMP-2 was evident, possibly due to larger spectrum of MMPs activating

MMP-2 than MMP-9. Treatment of cells with PMA for 24 h caused a strong increase in active MMP-2/9 levels characterized by lytic bands at 72 kD and 92 kD respectively. Incubation with different concentrations of aloe emodin caused a decrease in PMA induced MMP-2/9 activity eventhough the extent of inhibition varied for MMP-2 and MMP-9 (Figure 44, 45).

Figure 44. Inhibition of gelatinolytic activity by aloe emodin

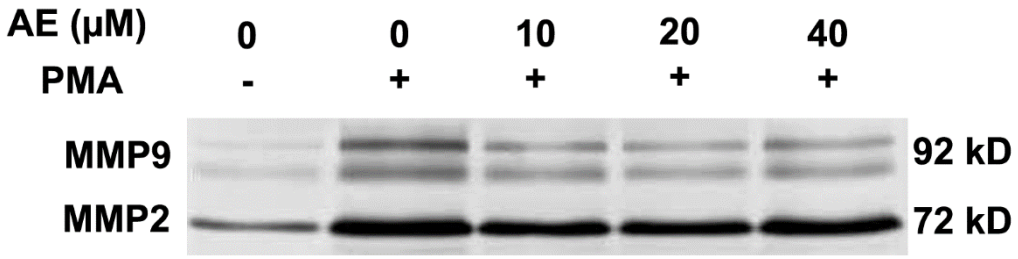

Cells were treated with 100 ng/ml PMA and different concentrations of aloe emodin for 24 h. Subsequently, the conditioned medium was collected, concentrated using amicon ultra centrifuge tubes (10 kD cutoff) and samples were electrophoresed on 8% SDS-polyacrylamide gel containing 0.1% gelatin, stained with Coomassie blue R-250. The result was confirmed independently by three experiments.

Figure 45. Fold change of gelatinolytic activity by aloe emodin

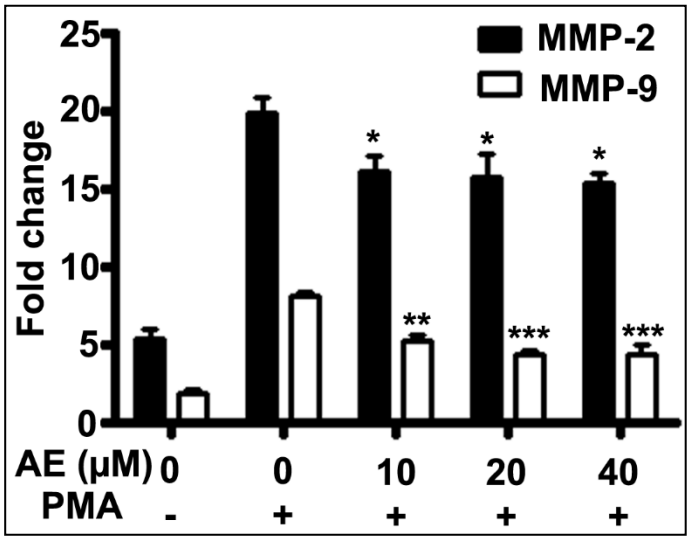

Non-staining bands representing the levels of the active form of MMP-2 and MMP-9 were quantified by densitometric measurement. Fold change of the gelatinase activity at varying

*concentration of aloe emodin treatment was plotted as a graph. Each value is presented as the mean ± SD of determinations from three independent experiments. The mean fold change was significantly lower than the corresponding PMA treated group as analyzed by Student's t-test. *P < 0.05; **P < 0.01; ***P < 0.001.*

Aloe emodin represses mRNA and protein expression of RhoB

Cancer cell migration/invasion is regulated by a variety of molecules involved in various signaling, matrix digestion and cytoskeletal reorganization, among which Rho family of proteins are the important one. On analysis of mRNA expression of Rho family of genes after treatment with aloe emodin, we observed a 2.6 fold repression in RhoB mRNA levels in semiquantitative RT-PCR analysis (Figure 46, 47).

Figure 46. SQRT-PCR of RhoB expression in aloe emodin treated cells

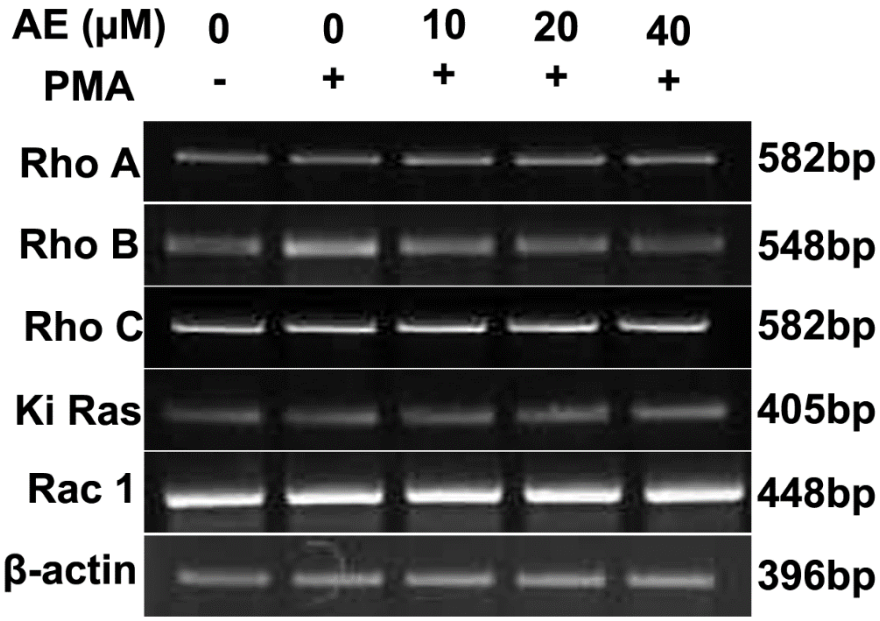

RNA was isolated and reverse transcribed into cDNA and then amplified by using specific primers. The amplified PCR products were electrophoresed on 2% agarose gel and documented. The experiment was repeated three times with similar results.

Figure 47. Fold change of RhoB mRNA expression in aloe emodin treated cells

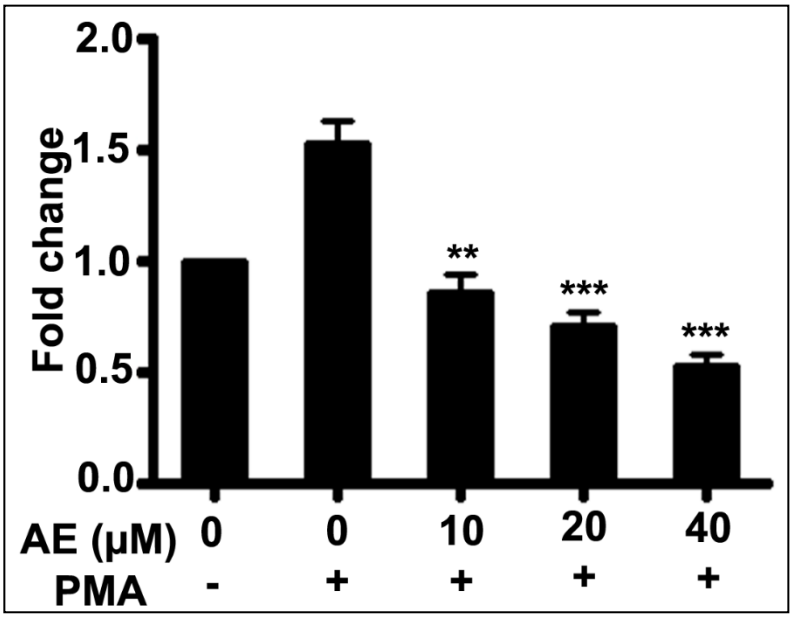

*Fold change of the RhoB mRNA expression, analyzed by Semi Quantitative RT- PCR at varying concentration of aloe emodin treatment was normalized with that of β-actin and was plotted as a graph. Each value is presented as the mean ± SD of determinations from three independent experiments. The mean fold change was significantly lower than the corresponding PMA treated group as analyzed by Student's t-test. *P < 0.05; **P < 0.01; ***P < 0.001.*

The results were further confirmed by using Real Time RT-PCR analysis. Treatment of aloe emodin reduced the expression of RhoB mRNA by 2.9 fold (Figure 48). These results evidently indicate the involvement of RhoB in antimigratory property of aloe emodin.

Figure 48. Real Time RT-PCR analysis of RhoB inhibition by aloe emodin

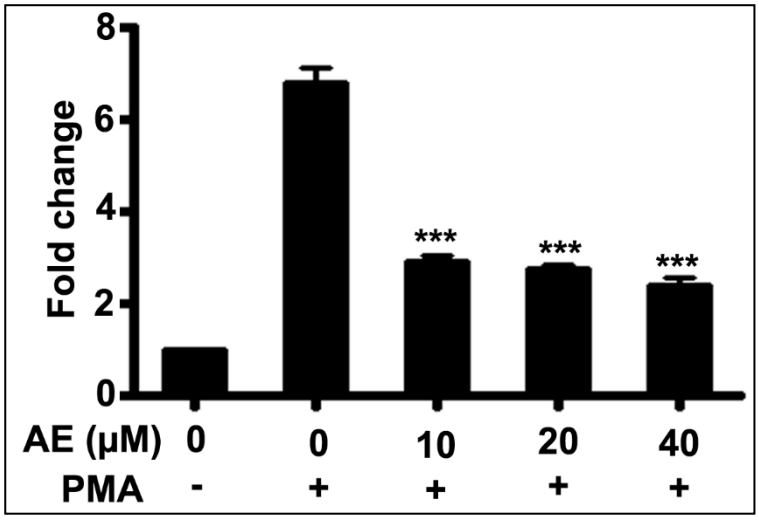

*The real- time PCR was performed in 7900 HT Fast Real- Time PCR system using MESA green qPCR Mastermix for SYBR Assay. Fold change of the target mRNAs were normalized with that of β-actin and is plotted as a graph. Each value is presented as the mean ± SD of determinations from two independent experiments. The mean fold change was significantly lower than the corresponding PMA treated group as analyzed using One-way ANOVA followed by Tukey's post hoc t- test analysis. ***P< 0.001.*

To determine whether downregulation in RhoB transcription was associated with decreased promoter activity we performed a reporter plasmid assay for RhoB promoter activity. For that we used luciferase reporter plasmid with RhoB promoter sequence -282 to +313 bp from the transcription start site cloned on to pGL2 basic vector (pGL2-RhoB-luc). This promoter portion consists of multiple binding sites for transcription factors including Ap-2, Sp-1, which ensures a sufficient level of RhoB promoter activation in untreated cancer cells. PMA activated RhoB expression by 6.7 fold which was brought down to that of control by 20 µM of aloe emodin treatment (Figure 49).

Figure 49. Aloe emodin inhibits RhoB promoter activity

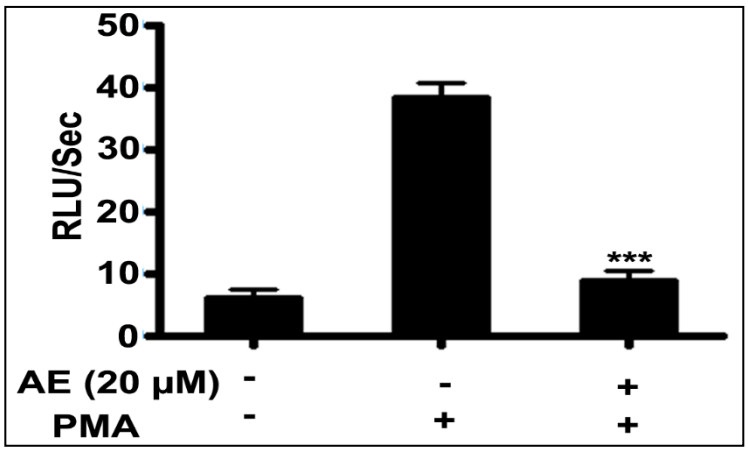

*The cells were transfected with pRL-Null, RhoB luciferase reporter plasmids and treated with and without aloe emodin/PMA. Luciferase reporter assay was performed by Dual Luciferase Reporter Assay System following the manufacturer's instruction. The relative luminescence units were normalized with the pRL-Null activity /protein content. Each value was presented as the mean ± SD of determinations from two independent experiments. The mean RLU of aloe emodin treated sample was significantly lower than the corresponding PMA treated group as analyzed using One-way ANOVA followed by Tukey's post hoc t- test analysis. ***P < 0.001.*

Next we analyzed the change in expression of RhoB protein on treatment with aloe emodin. Our result clearly shows that 20 and 40 µM of aloe emodin decreased RhoB expression by 2.5 fold (Figure 50, 51).

Figure 50. Aloe emodin inhibits RhoB protein expression

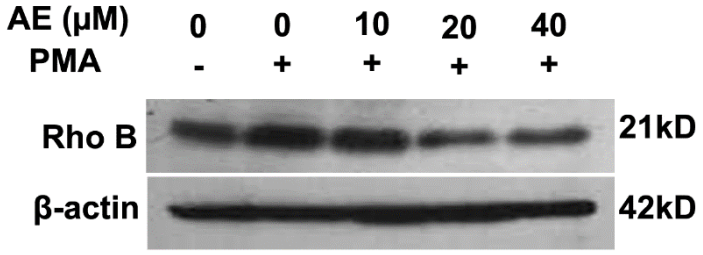

Cells were treated with indicated concentrations of aloe emodin/PMA for 24 h. The cell lysates were evaluated for RhoB expression by Western blotting. The above experiment was repeated three times with similar results.

Figure 51. Fold change of RhoB protein in aloe emodin treated cells

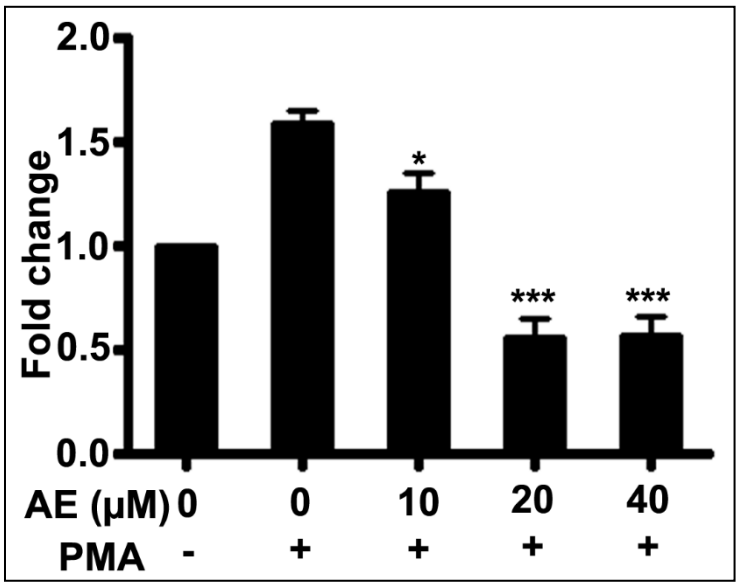

*Fold change of the RhoB protein expression, analyzed by Western blot at varying concentrations of aloe emodin treatment was normalized with that of β-actin and was plotted as a graph. Each value is presented as the mean ± SD of determinations from three independent experiments. The mean fold change was significantly lower than the corresponding PMA treated group as analyzed by Student's t-test. *P < 0.05; **P < 0.01; ***P < 0.001.*

In summary, we have shown aloe emodin indeed brings down the mRNA levels of matrix digesting enzymes, MMP-2/9 and cell motility regulating protein, RhoB by transcriptional regulation. Decreased gelatinolytic activity in the culture supernatant and decreased RhoB protein expression was also seen upon treatment with aloe emodin.

Aloe emodin blocks PMA induced ERK1/2 phosphorylation and NF-κB-DNA binding

ERK1/2 is known to control the expression of several transcription factors like AP-1, NF-κB, which in turn has been implicated in the induction of several MMPs expression (Sato et al., 1993, Gum et al., 1996, Eberhardt et al., 2002, Takahra et al., 2004). Therefore we analyzed the regulation of PMA induced MAP kinases on treatment with aloe emodin.

Aloe emodin prevents PMA induced phosphorlyation of ERK1/2

Treatment of cells with PMA augmented phosphorylation of ERK1/2 which was reversed by different concentrations of aloe emodin. JNK1/2 also gets activated in presence of PMA, but aloe emodin fails to inhibit the PMA induced JNK1/2 activation. In fact, there was an overall activation of JNK1/2 after aloe emodin treatment alone (Figure 52, 53).

Figure 52. PMA induced pERK1/2, pJNK1/2 expression by aloe emodin

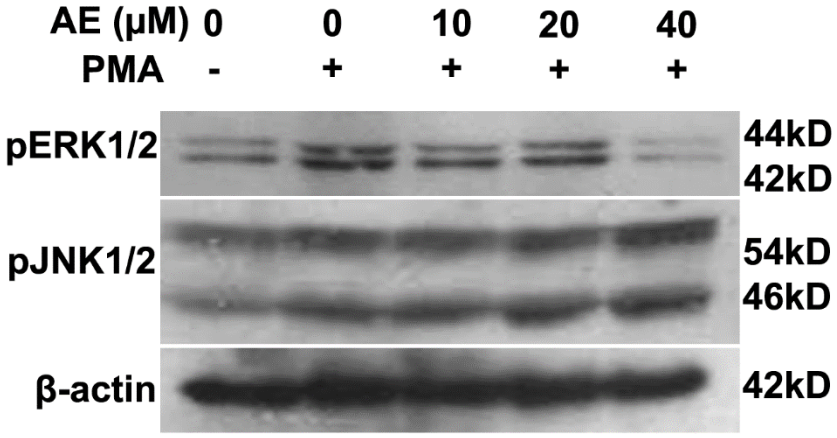

Serum starved cells were treated with PMA followed by different concentrations of aloe emodin for 12 h. The cell lysates were evaluated for levels of pERK1/2, pJNK1/2 expression by Western blotting

Figure 53. Fold change of pERK1/2 and pJNK1/2 in aloe emodin treated cells

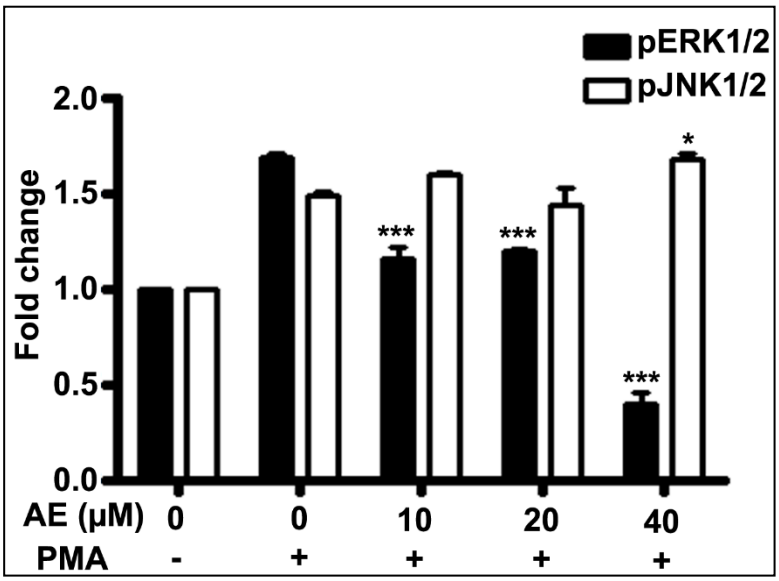

*Fold change was normalized with that of β-actin and was plotted as a graph. Each value is presented as the mean ± SD of determinations from three independent experiments. The mean fold change was significantly lower than the corresponding PMA treated group as analyzed using One-way ANOVA followed by Tukey's post hoc t- test analysis. *P < 0.05; ***P < 0.001.*

Aloe emodin inhibits PMA induced NF-κB-DNA binding

NF-κB proteins comprise a family of transcription factors that are involved in the control of a large number of cellular processes, such as cellular growth and apoptosis. In addition, these transcription factors are persistently active in a number of diseases, including cancer. To test whether aloe emodin interferes with the DNA-binding activity of NF-κB we performed EMSA. Stimulation of cells with PMA (100 ng/ml) caused enhancement in the binding of proteins to NF-κB specific oligonucleotides, whereas treatment with aloe emodin caused inhibition of such binding. We did not get any reduction in the binding activity of AP-1 on treatment with aloe emodin. This result suggests that NF-κB pathway is important in aloe emodin induced MMP down regulation (Figure 54).

Figure 54. DNA binding activity of NF-κB/ AP-1 on treatment with aloe emodin

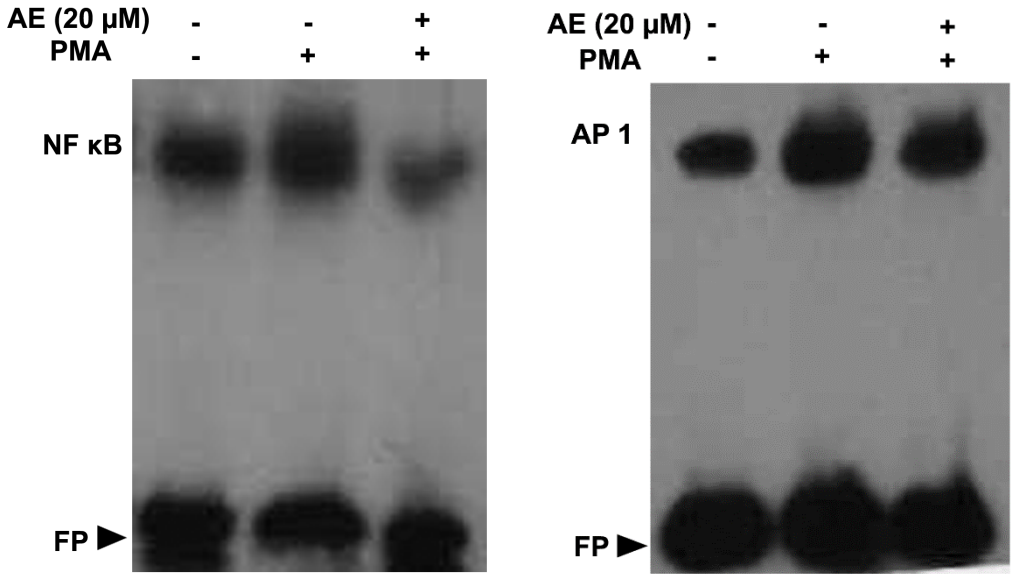

WiDr cells were incubated with aloe emodin for 4 h with or without PMA. Nuclear extracts were prepared and assayed for NF-κB/AP-1-DNA binding using EMSA.

Effect of aloe emodin on nuclear translocation of NF-κB subunits p65/p50

The transcription factor NF-κB consists of homo- or heterodimers of different subunits. Five different NF-κB protein subunits have been identified so far, p50, p52, p65, RelB, and c-Rel. p50, is synthesized as a large precursor p105 which undergo proteolytic processing to generate mature NF-κB subunit p50. p50 and p65 (RelA) were the first NF-κB subunits to be identified and proved to be an active heterodimer involved in the transcriptional regulation of most of the genes. From the study so far, aloe emodin was shown to inhibit the DNA binding activity of NF-κB but not AP1. Our next aim was to analyze the whether reduction in DNA binding activity of NF-κB is due to decreased nuclear translocation of NF-κB subunits p65/p50 and whether aloe emodin has any role in nuclear translocation of these NF-κB subunits. Treatment of PMA induced the translocation of both p65 and p50 subunits into the nucleus. Western blot analysis of nuclear proteins have shown that aloe emodin could inhibit PMA induced nuclear translocation of p50, its precursor p105 and p65 subunits. Even though nuclear p65/p50 levels were inhibited by aloe emodin, the extent to which it inhibited these proteins differed and p50 was relatively more inhibited than p65 (Figure 55, 56).

Figure 55. Inhibition of PMA induced nuclear translocation of NF-κB subunits by aloe emodin

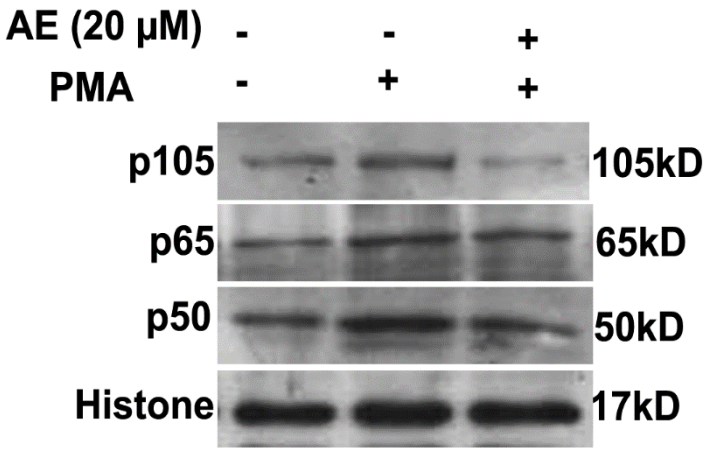

Cells were treated with PMA/aloe emodin for 4 h. The nuclear lysates were evaluated for p105/p65/p50 proteins by Western blotting as described in Materials and Methods.

Figure 56. Fold change of nuclear translocated NF-κB subunits on aloe emodin treatment

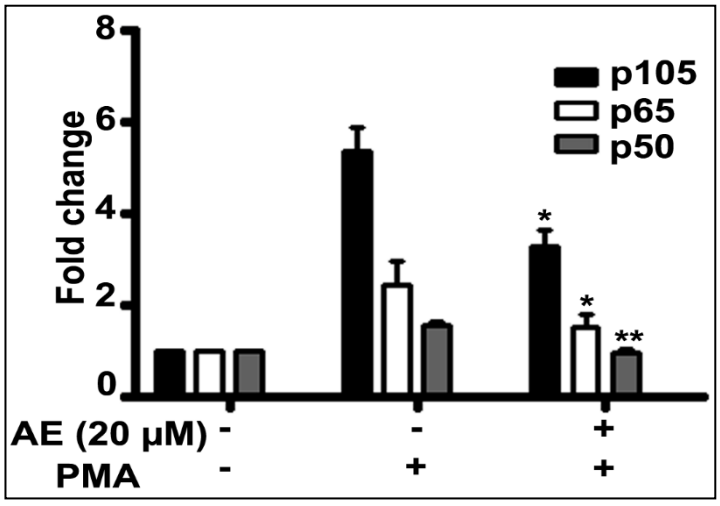

*Fold change of the NF-κB subunits, p105, p50, p65, on aloe emodin treatment was normalized with that of histone and was plotted as graph. Each value is presented as the mean ± SD of determinations from two independent experiments. The mean fold change was significantly lower than the corresponding PMA treated group as analyzed by Student's t-test. *P < 0.05; **P < 0.01.*

However, there was no change in the cytoplasmic IκB levels when treated with aloe emodin (Figure 57).

Figure 57. PMA induced IκB expression by aloe emodin

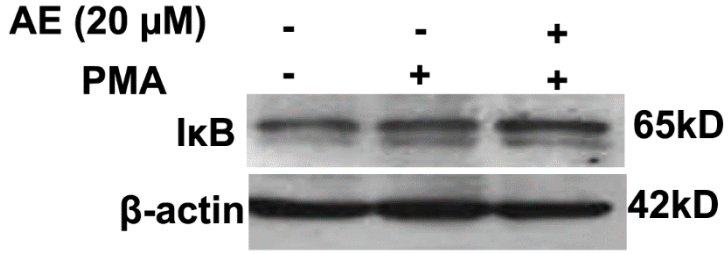

Cells were treated with PMA/aloe emodin for 4 h. The cytoplasmic lysates were evaluated for IκB by Western blotting. The experiment was repeated at least two times with similar results.

In summary, the results suggest that aloe emodin inhibits PMA-induced ERK phosphorylation, DNA binding of NF-κB via downregulation of nuclear levels of p50 and p65 subunits.

D) Inhibition of angiogenesis by aloe emodin

Angiogenesis plays an important part in the process of metastasis and is seen along with tumor progression. When solid cancers are small, they are supplied with nutrients by diffusion from nearby blood vessels. In order to grow larger, they need their own blood vessels, which they create by increased angiogenesis by producing angiogenic factors such as VEGF. Drugs that interrupt this process show promise in treating cancer. Our findings showed aloe emodin inhibits Human Umbilical Vein Endothelial cells (HUVECs) proliferation, migration/invasion and in vitro tube formation. We have also analyzed its effects on VEGF expression.

Aloe emodin inhibits VEGF-A expression and promoter activity in tumor cells

Angiogenesis plays an important part in the process of metastasis and is seen along with tumor progression. Since VEGF-A plays a key role in prompting angiogenesis, we assayed mRNA levels of VEGF-A in aloe emodin treated cells by semi quantitative RT-PCR. The results show that expression of VEGF-A in WiDr cells was inhibited by varying concentrations of aloe emodin (Figure 58, 59).

Figure 58. SQRT-PCR of VEGF expression in aloe emodin treated cells

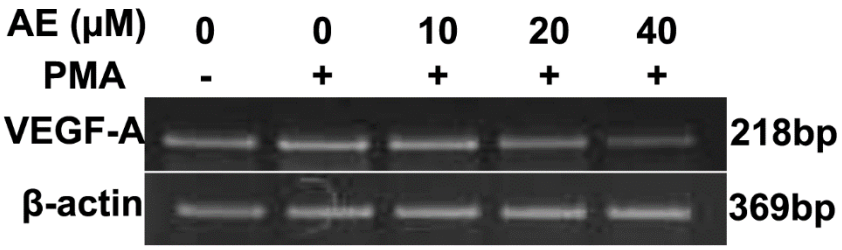

RNA was isolated and reverse transcribed into cDNA and then amplified by using specific primers. The amplified PCR products were electrophoresed on 2% agarose gel and documented. The experiment was repeated three times with similar results.

Figure 59. Fold change of VEGF-A mRNA in aloe emodin treated cells

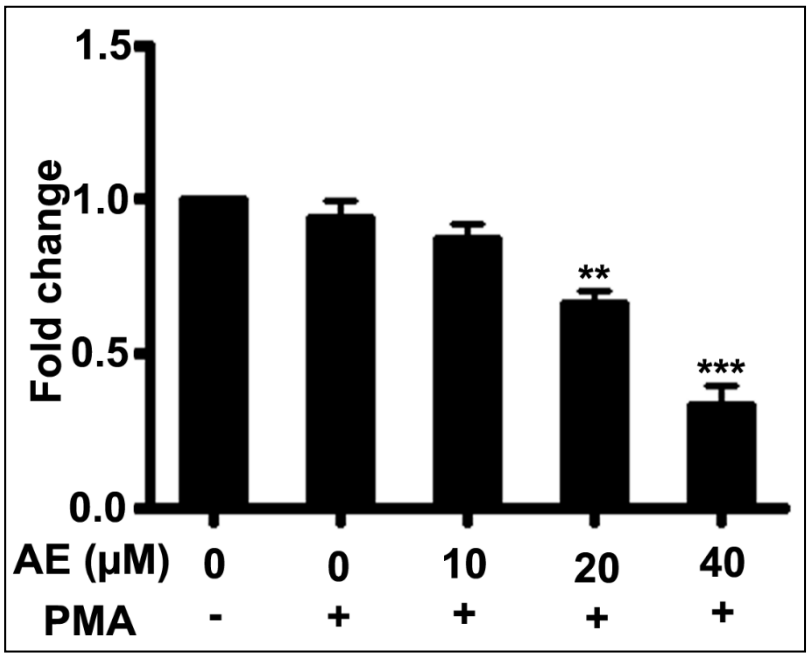

*Fold change of the VEGF-A mRNA expression, analyzed by Semi Quantitative RT- PCR at varying concentration of aloe emodin treatment was normalized with that of β-actin and was plotted as a graph. Each value is presented as the mean ± SD of determinations from three independent experiments. The mean fold change was significantly lower than the corresponding PMA treated group as analyzed by Student's t-test. **P < 0.01; ***P < 0.001.*

We also confirmed this by Real Time RT-PCR which showed that aloe emodin treatment decreased PMA induced VEGF-A mRNA by more than 7 fold on treatment with 40 µM aloe emodin (Figure 60).

Figure 60. Real Time RT-PCR of VEGF-A inhibition by aloe emodin

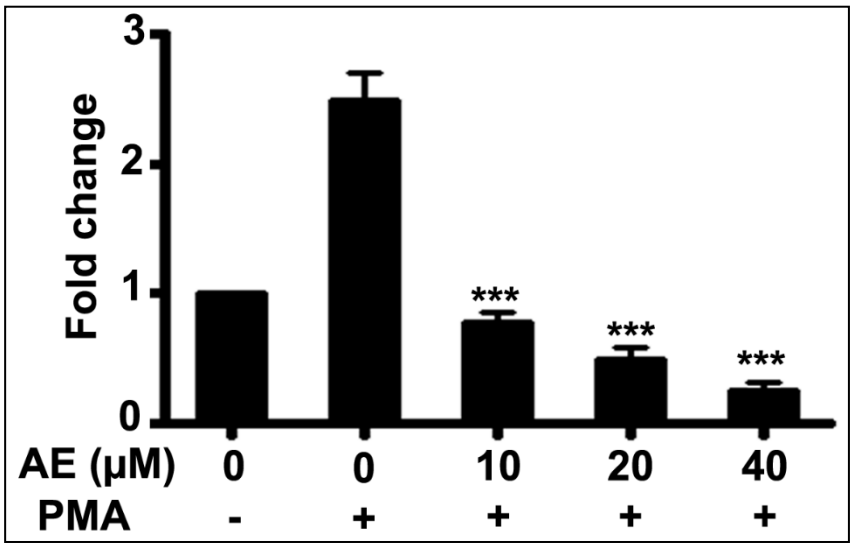

*The real- time PCR was performed in 7900 HT Fast Real- Time PCR system using MESA green qPCR Mastermix for SYBR Assay. Fold change of the VEGF-A mRNA was normalized with that of β-actin and was plotted as a graph. Each value is presented as the mean ± SD of determinations from two independent experiments. The mean fold change was significantly lower than the corresponding PMA treated group as analyzed using One-way ANOVA followed by Tukey's post hoc t- test analysis. ***P < 0.001.*

Effect of aloe emodin on PMA induced VEGF-A promoter activity

Here we evaluated whether the transcriptional control of VEGF-A expression was due to the regulation of promoter activity by using luciferase reporter assay. Luciferase reporter plasmid containing gene spanning -1176 /+54 region of VEGF promoter, constructed in pGL2 basic vector (pGL2-VEGF-Luc) was used to investigate and the results show that aloe emodin treatment brought down the transcriptional activity of VEGF-A promoter to the basal level (Figure 61). This finding noticeably indicates the probable role of aloe emodin as antiangiogenic agent.

Figure 61. Inhibition of VEGF-A promoter activity by aloe emodin

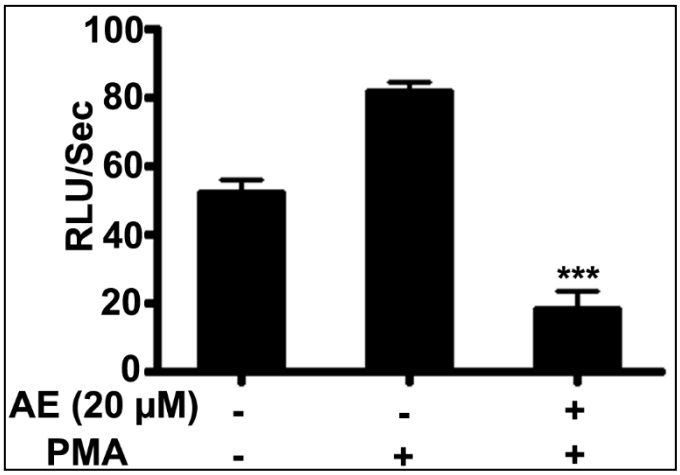

*The cells were transfected with pRL-Null, VEGF-Luciferase reporter plasmids and treated with and without aloe emodin/PMA. Luciferase reporter assays were performed by Dual Luciferase Reporter Assay System following the manufacturer's instruction. The relative luminescence units were normalized with the pRL-Null activity /protein content. Each value is presented as the mean ± SD of determinations from three independent experiments. The mean RLU of aloe emodin treated sample was significantly lower than the corresponding PMA treated group as analyzed using One-way ANOVA followed by Tukey's post hoc t- test analysis. ***P < 0.001.*

Aloe emodin inhibits proliferation of HUVECs

In vitro antiangiogenic assays were carried out in HUVECs to test the specific effect of aloe emodin on several key steps of the angiogenic process which include endothelial cell proliferation, migration/invasion and *in vitro* tube formation. Local proliferation of endothelial cells is the first step in the angiogenic process. Results showed that aloe emodin exhibited a concentration dependent antiproliferative activity on HUVECs (Figure 62).

Figure 62. Analysis of cell viability in aloe emodin treated HUVECs

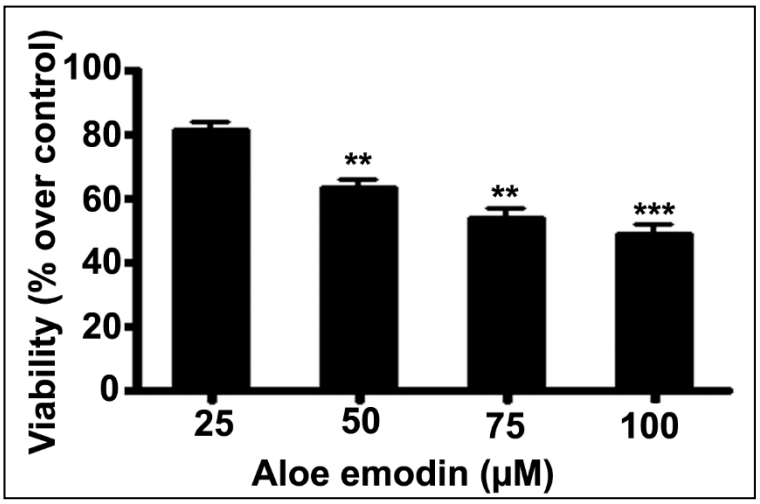

*Cells were treated with or without the indicated concentrations of aloe emodin for 48 h. At the end of treatment, cell viability was assessed by MTT assay. All results were expressed as the mean percentage of control ± S.D. of quadruplicate determinations from three independent experiments. The differences among the mean values were analyzed using One-way ANOVA followed by Tukey's post hoc t- test analysis. The One-way ANOVA revealed that the average mean values of cell survival differed significantly as a function of concentration of aloe emodin. **P < 0.01; ***P < 0.001.*

Aloe emodin inhibits *in vitro* cell migration/invasion of HUVECs

A relatively non toxic concentration (25 µM) of aloe emodin was chosen for analysing its effect on transwell migration/invasion and *in vitro* tube formation assay. Inhibitory effect of aloe emodin on endothelial cell migration/invasion was analyzed by modified Boyden's chamber assay. Endothelial cells with high migratory ability can only pass through the membrane of 8 µm pore. Aloe emodin (25 µM) effectively diminished the migratory ability of endothelial cells through the porous inserts (Figure 63).

Figure 63. Inhibition of transwell migration of endothelial cells by aloe emodin

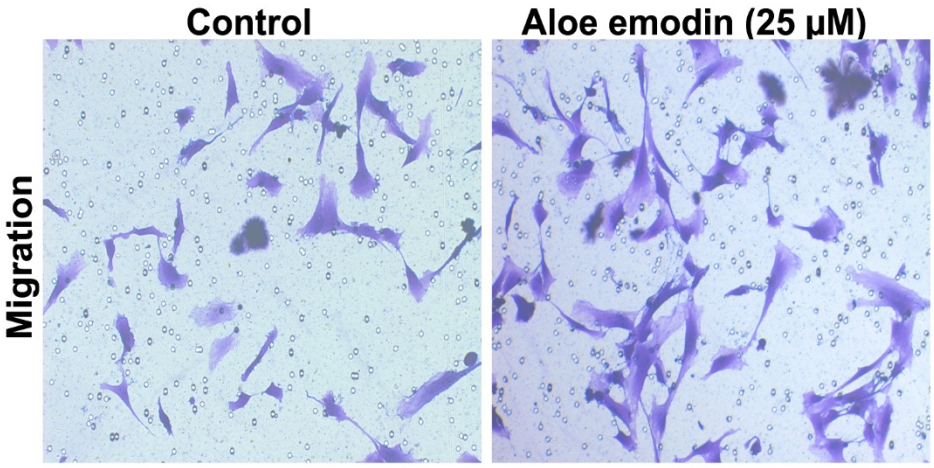

Migration of endothelial cells was determined with modified Boyden's chamber method. Response of cells for aloe emodin was assayed using 24-well migration chamber with an upper well having a membrane of 8 µm pore and 12 mm of diameter. Cells on the upper side of the membrane were carefully removed by using a wet cotton swab after incubation with aloe emodin/PMA and migrated cells were stained with crystal violet and counted.

Aloe emodin was also shown to inhibit invasive ability of HUVECs through matrix coated membranes, the extent of inhibition was found to be 3 fold in both cases (Figure 64, 65).

Figure 64. Inhibition of transwell invasion of endothelial cells by aloe emodin

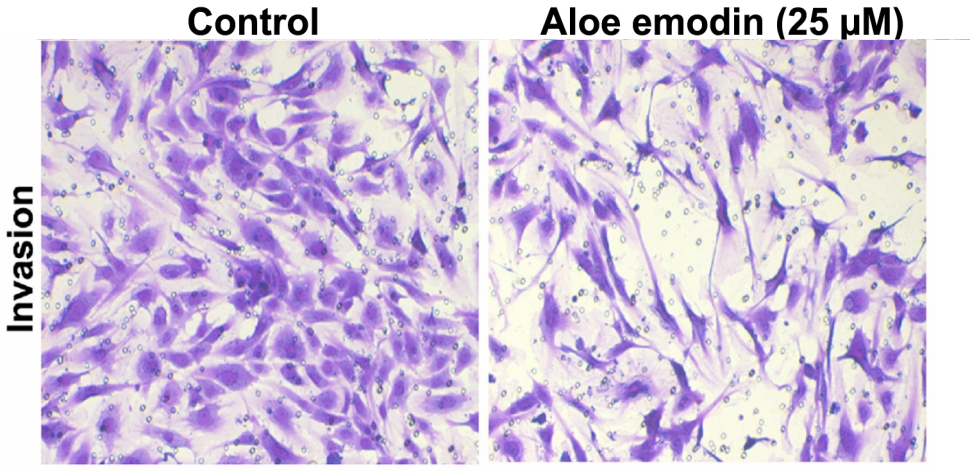

In case of assessing cell invasion BioCoat Martigel Invasion Chambers were used. Response of cells for aloe emodin was assayed using 24-well migration chamber with an upper well having a membrane of 8 µm pore coated with Matrigel. Cells on the upper side of the membrane

were carefully removed by using a wet cotton swab after incubation with aloe emodin/PMA and migrated cells were stained with crystal violet and viewed.

Figure 65. Inhibition of transwell migration/invasion by HUVECs cells on aloe emodin treatment

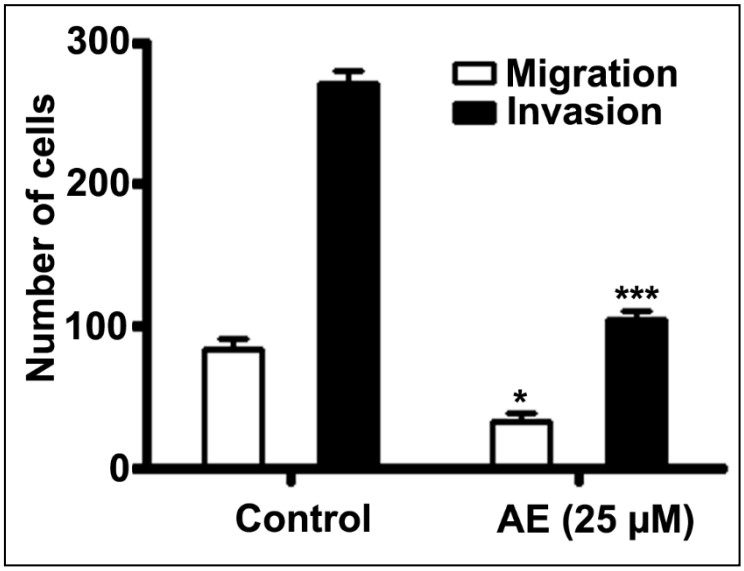

*Migration of HUVECs was determined with modified Boyden's chamber method. The experiment was repeated three times with similar results and the number of cells migrated/invaded was counted and plotted in the graph. The mean number of cells was significantly lower in the aloe emodin treated sample as analyzed by Student's t-test. Bars indicate S.D. *P < 0.05; **P < 0.01.*

Aloe emodin inhibits *in vitro* tube formation of HUVECs

The final event during angiogenesis is the organization of endothelial cells in a three-dimensional network of tubes. HUVECs align themselves in a three-dimensional tube like network when plated on matrigel. Figure 66 showed that the treatment with 25 μM of aloe emodin for 24 h significantly inhibited tube formation of HUVEC on matrigel.

Figure 66. *In vitro* tube formation assay

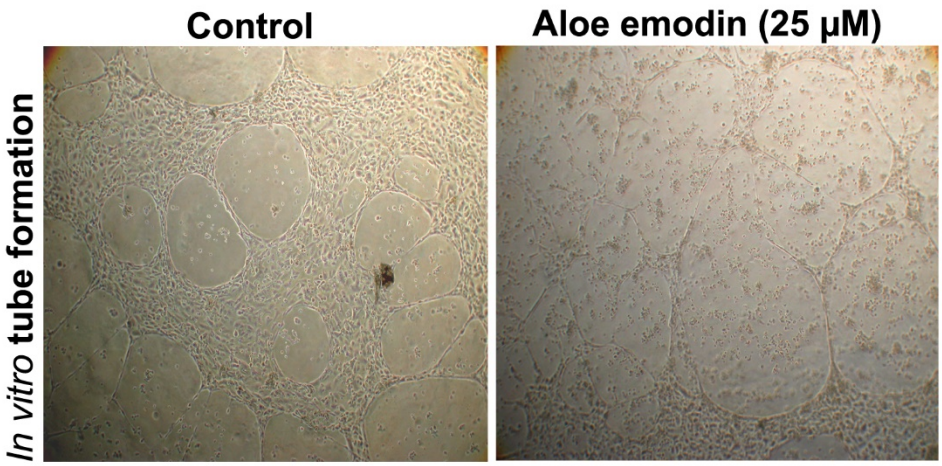

HUVECs were plated on the Matrigel and cultured in DMEM with and without aloe emodin for 24 h. The enclosed network of complete tubes/incomplete structures were observed and photographed under light microscope. Results were confirmed by two independent experiments.

In summary, we have shown aloe emodin indeed brings down the mRNA levels of potent angiogenic inducer VEGF-A and it does so by transcriptional inhibition in tumor cells. Aloe emodin was also shown to inhibit crucial events in angiogenic process such as proliferation, migration/invasion and *in vitro* tube formation of HUVECs.

Based on the experimental evidence obtained from our *in vitro* studies using tumor cells/ HUVECs, a schematic representation of pathways activated / inhibited is provided in Figure 67.

Figure 67. Schematic diagram illustrating the proposed inhibitory mechanism of aloe emodin

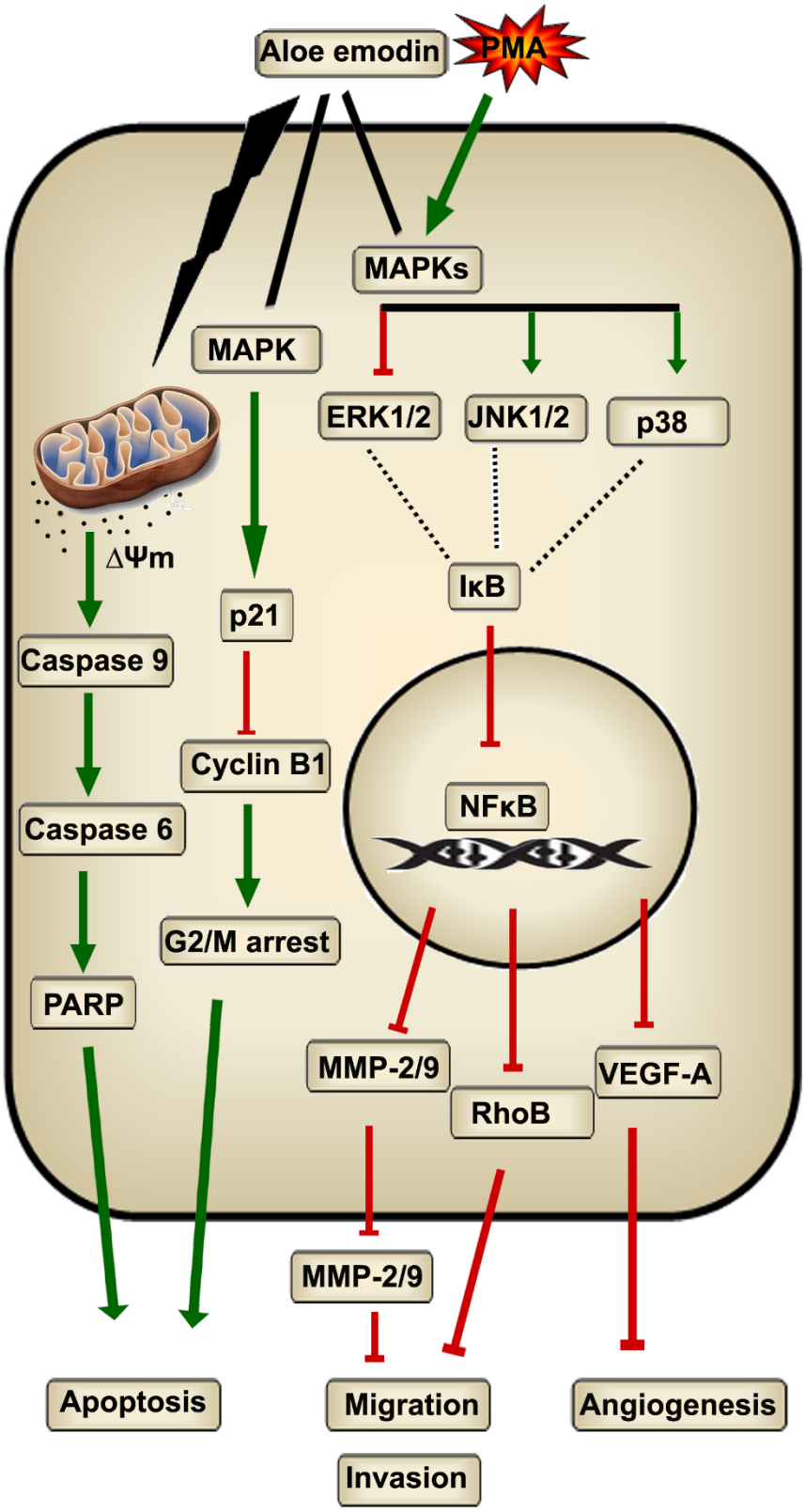

Aloe emodin inhibits ERK1/2 phosphorylation and activates JNK1/2 and p38, which leads to cell cycle arrest at G2/M phase via reducing the expression of cyclin B1. Loss in the mitochondrial membrane potential in aloe emodin treatment activates caspase -9 followed by caspase -6 which culminates in apoptotic cell death. Aloe emodin downregulates the nuclear translocation, DNA binding of NF-κB and also inhibits MMPs and RhoB activities at both mRNA and protein levels leading to reduced migration and invasion. In vitro angiogenesis was also inhibited by aloe emodin by reducing expression of VEGF-A and promoter activity. Green arrows denote activator pathways and red blunted lines show inhibitory pathways. Black dotted arrows shows pathways with multiple partners and black line/arrow represent involvement of these pathways.

16. Science and Technology benefits accrued:

a. List of Research publications with complete details: 3

1. **Gopal Srinivas**, Suboj Babykutty, Priya Prasanna Sathiadevan, Priya Srinivas. Molecular mechanism of emodin action: transition from laxative ingredient to an antitumor agent. ***Med Res Rev,*** 27 (5): 591- 608, 2007.
2. Priya S, Suboj Babykutty, Priya Srinivas, **Srinivas Gopala**. Aloe emodin induces G2/M cell cycle arrest, and apoptosis via activation of caspase- 6 in human colon cancer cells. ***Pharmacology*** 89: 91-98, 2012.
3. Priya S, Suboj Babykutty, Deepak Roshan V G, Rakesh S Nair, Priya Srinivas, **Srinivas Gopala**. Aloe emodin inhibits colon cancer cell migration/angiogenesis by downregulating MMP-2/9, RhoB and VEGF via reduced DNA binding activity of NF-κB. ***European Journal of Pharmaceutical Sciences*** 45: 581-591, 2012.

Papers presented in symposiua/ conferences:

1 Priya Prasanna Sathiadevan, Suboj Babykutty, Vinod Vijayakurup, Priya Srinivas, Gopal Srinivas. In vitro anticancer activity of aloe emodin involves G2/M arrest and inhibition of metastasis in colon cancer cells. P41. International PSE symposium on natural Products and Cancer Therapy, Naples, Italy, 2008.

2 Priya Prasanna Sathiadevan Suboj Babykutty, Vinod Vijayakurup, Padmakrishnan.C.J, Priya Srinivas, Srinivas Gopala. Aloe emodin, a natural anthraquinone targeting multiple facets (migration, invasion, angiogenesis) of tumor metastasis. ECCO 15 - 34th ESMO Multidisciplinary Congress. Berlin, 2009.

Manpower trained on the project:

i. Research Scientists or Research Associates : Nil

ii. No. of PhD's produced : **2**

iii. Other Technical Personnel trained : nil

c. Patents taken, if any : Nil

d. Products developed, if any : Nil

17. Procurement of/Usage of Equipment:

a. Details of Equipment:

Sl.No.	Name of equipment	Make/Model	Cost (Rs.)	Date of Installation	Utilisation	Remarks regarding maintenance breakdown
1	Inverted Microscope	Olympus IX-51	2.5 Lakhs	Dec 2005	100%	Working

b. Suggestions for disposal of equipment(S): Microscope in use now

(Name and Signature of PI)